Tropical Cyclogenesis via Convectively Forced Vortex Rossby Waves in a Shallow Water Primitive Equation Model

JANICE ENAGONIO AND MICHAEL T. MONTGOMERY

Department of Atmospheric Science, Colorado State University, Fort Collins, Colorado

(Manuscript received 23 July 1999, in final form 30 May 2000)

ABSTRACT

This work examines further the problem of tropical cyclogenesis by convective generation of vertical vorticity within a preexisting cyclonic circulation whose initial maximum tangential wind is approximately 5 m s^{-1}. This paper validates and extends recent work examining the suggested upscale cascade mechanism in a three-dimensional quasigeostrophic framework using a simple shallow water primitive equation (SWPE) numerical model and helps clarify certain aspects of the Rossby adjustment problem on a nonresting basic state for finite-amplitude nonaxisymmetric disturbances. The SWPE approach serves as a meaningful intermediate step between the quasigeostrophic and full-physics frameworks and allows a simple investigation of the effects of unbalanced dynamics (contributions of gravity waves) and Rossby numbers of order unity.

The authors compare quantitative results of the two models on the storm spinup time and magnitude. For asymmetric initial conditions whose mass and wind field are out of balance, robust spinup is still obtained provided the initial asymmetries possess a significant vortical component. Episodic convective forcing parameterized via unbalanced vorticity anomalies is shown to lead to spinup of a tropical storm strength vortex on a timescale of approximately 40 h.

When the convective vorticity anomaly has a large amplitude compared to the initial 5 m s^{-1} basic-state vortex, the convective anomaly becomes the dominant or ''master vortex,'' remaining essentially intact and shearing the basic-state vortex. This behavior is understood heuristically in terms of a ''vortex beta Rossby number,'' which provides a local measure of the strength of the nonlinear terms in the vorticity equation compared to the corresponding linear vortex Rossby wave restoring term.

Additional experiments show that, if the convection in a single pulse mode occurs in multiple patches (or ''subclusters'') rather than in a single cluster with equal cyclonic circulation, a reduced spinup is obtained. This effect is captured in simulations with a nonlinear nondivergent semispectral model, establishing that gravity wave dynamics are not responsible for the reduction of spinup in the multiple-cluster case. A wave-mean-flow approximation with the nondivergent model also reproduces the effect of a reduced spinup with multiple-cluster convection. The applicability of the wave-mean-flow approximation at these finite amplitudes is explained by the fact that the vortex beta Rossby number of these configurations is not large.

A case study using satellite observations shows that, although the observations are for a tropical storm rather than for genesis, an intensification mechanism similar to that discussed here is suggested. Further tests of the theory are proposed.

1. Introduction

The majority of tropical cyclones form from tropical cloud clusters or mesoscale convective systems over the tropical oceans under favorable climatological conditions (Gray 1968; Zehr 1992). Most such disturbances, even given favorable climatological conditions, fail to develop into tropical cyclones. Much research has been devoted to the problem of determining what further conditions bring about tropical cyclogenesis, here defined as the growth of an incipient cyclonic vortex into an organized rotary circulation possessing a warm core thermal structure and tangential winds that decrease with height.

This paper builds on the research by Montgomery and Enagonio (1998, hereafter ME), which indicated that, given favorable climatological conditions, mesoscale/synoptic-scale processes leading to an incipient vortex (such as a mesoscale convective vortex or cyclonic closed flow pattern in an easterly wave) combined with vorticity sources produced by episodes of deep moist convection near or within the radius of maximum tangential wind (RMW) of the vortex would lead to tropical cyclone formation. The vertical motion and thermal structure of the evolving vortex were also studied, and it was shown that a warm core forms as a natural consequence of vortex axisymmetrization processes described by quasigeostrophic balanced dynamics. The

Corresponding author address: Dr. Michael T. Montgomery, Department of Atmospheric Science, Colorado State University, Fort Collins, CO 80523-1371.
E-mail: mtm@charney.atmos.colostate.edu

limitations of the ME study were that the dynamics was restricted to be quasigeostrophic and that the wind and height fields of the convective potential vorticity (PV) disturbances were assumed to be in geostrophic and hydrostatic balance. In actuality neither of these conditions are strictly satisfied in the moist convective region of the incipient vortex: the standard Rossby number associated with the incipient vortex is generally $O(1)$ and the convective forcing produces vorticity that is generally not in balance with the mass field.

The purpose of the present paper is to determine the extent to which the quasigeostrophic predictions are still valid for order unity Rossby numbers and for unbalanced convective forcing. Since the length scales of the cyclogenesis problem (~100 km) are small compared to the ambient radius of deformation for tropopause depth-scale disturbances (~1000 km in the Tropics), and the Froude number is much less than one, the problem is barotropic to leading order (McWilliams 1985). The shallow water primitive equation (SWPE) calculations are thus relevant to the cyclogenesis problem and provide a simple framework in which to investigate the issues of unbalanced dynamics (i.e., the importance of gravity waves) and order unity Rossby number. The SWPE simulations define an intermediate step between balanced quasigeostrophic dynamics and the fully three-dimensional primitive equations, the latter of which includes unbalanced aspects, the secondary circulation, and vortex alignment dynamics.[1] The quasigeostrophic results are extended here to configurations with stronger convective vortices and multiple clusters of convection.

The primitive equation results are also compared to the results of a semispectral model, which solves the nondivergent vorticity equation. The semispectral model is used to assess the quasilinear, wave-mean-flow and fully nonlinear levels of accuracy in the ensuing vorticity dynamics (see section 2b). The observed applicability of the wave-mean-flow approximation at the large vorticity amplitudes employed here is explained heuristically using a vortex ''beta Rossby number,'' which provides a local measure of the initial importance of nonlinear versus linear terms in the vorticity equation.

Convective asymmetries in tropical storm and hurricane-strength tropical cyclones have been observed and studied sporadically over the past 30 yr (Soules and Nagler 1969; Gentry et al. 1970; Black et al. 1986; Marks et al. 1992; Gamache et al. 1993; Molinari et al. 1999), and the idea of intensification of a tropical cyclone by asymmetric convection is not new. Only recently, however, has a simple dynamical framework for understanding vortex intensification by asymmetrization processes been developed (Montgomery and Kallenbach 1997). This idea has been investigated in greater detail by ME, Enagonio and Montgomery (1998), and Möller and Montgomery (1999, 2000). These papers are an outgrowth of the vortex axisymmetrization and vortex merger research of Melander et al. (1987a,b; 1988), McCalpin (1987), Carr and Williams (1989), Sutyrin (1989), Dritschel and Waugh (1992), Ritchie and Holland (1993, 1997), Holland and Dietachmayer (1993), Guinn and Schubert (1993), Smith and Montgomery (1995), Lansky et al. (1997), Bassom and Gilbert (1998, 1999), Nolan and Farrell (1999), and Schecter et al. (2000), which suggest that vortex ''axisymmetrization,'' or the tendency toward a state of circular flow on smoothly distributed vortices, is a universal process of quasi-two-dimensional vortex dynamics.

The outline of this paper is as follows. Section 2 describes the numerical models used in the present study and section 3 discusses the basic states and initializations used. Section 4 compares our primitive equation results to the quasigeostrophic results of ME. Section 5 presents further new results from the primitive equation model, including a study of the interaction of vortices of varying amplitudes based on vortex beta Rossby number ideas. Section 6 presents an example using satellite data suggesting vortex intensification due to a convective asymmetry. Section 7 summarizes the principle findings of this study and discusses further tests of the proposed theory.

2. The numerical models

a. The shallow water primitive equation model

The primary numerical model used for this work is a primitive equation finite-difference shallow water model in Cartesian coordinates (x, y) with a uniform resting depth, similar to Sadourny (1975) and Washington and Parkinson (1986). The model is designed to conserve potential enstrophy. In our implementation, potential enstrophy, area-integrated energy and PV are all conserved to within a fraction of a percent over the course of a typical model run. A Coriolis parameter of $f = 5 \times 10^{-5}$ s^{-1} is assumed for the simulations. In contrast to Sadourny, who used a damped leapfrog time-stepping scheme, a fourth-order Runge–Kutta scheme is employed. The model domain is 2000 km $\times$ 2000 km, with 400 $\times$ 400 grid points, yielding a grid spacing of 5 km in both the x and y directions. The coordinate system has $(x, y) = (0, 0)$ at the southwest corner of the domain. The complete prognostic equations are

[1] *Note added in proof:* Although simple scaling suggests that barotropic dynamics should suffice at leading order, the subtle dynamics of vortex co-rotation (which can frustrate axisymmetrization) and vortex alignment are not captured in this approximation (see Reasor and Montgomery 2001, in press, hereafter RM, and references therein). Work is under way to incorporate these aspects and the results will be reported in upcoming publications.

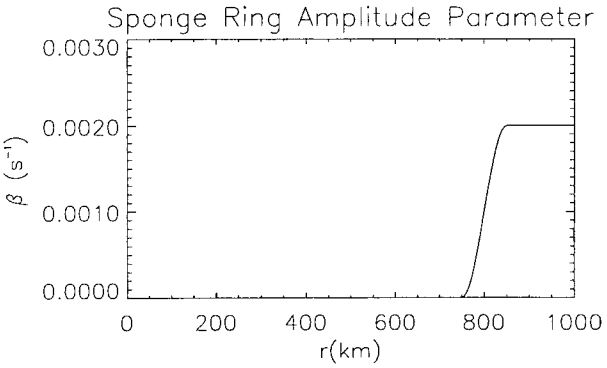

FIG. 1. Sponge ring profile $\beta(r)$ as a function of radius from the domain center.

$$\frac{\partial u}{\partial t} - \eta V + \frac{\partial H}{\partial x} + \nu_4\nabla^4 u + \beta(u - \overline{u}_0) = 0,$$

$$\frac{\partial v}{\partial t} + \eta U + \frac{\partial H}{\partial y} + \nu_4\nabla^4 v + \beta(v - \overline{v}_0) = 0, \quad \text{and}$$

$$\frac{\partial P}{\partial t} + \frac{\partial U}{\partial x} + \frac{\partial V}{\partial y} + \nu_4\nabla^4 P + \beta(P - \overline{P}_0) = 0.$$

Here u is the east–west zonal velocity, v the north–south meridional velocity, $P = gh$ is the geopotential, g is the gravitational acceleration, and h is the depth of the fluid. Here $U = Pu$ and $V = Pv$ are depth-integrated momenta and $H = P + \frac{1}{2}(u^2 + v^2)$ is the Bernoulli function. The potential vorticity η is given by

$$\eta = \frac{\partial v/\partial x - \partial u/\partial y + f}{P}.$$

A resting fluid depth of 1 km is chosen to give a maximum gravity wave speed of approximately 100 m s^{-1}, equal to the external gravity wave speed corresponding to the physical setup of ME, which had static stability $N = 10^{-2}$ s^{-1} and troposphere height $H = 10$ km. The Courant–Freidrichs–Lewy (CFL) condition implies a maximum time step of order 50 s; most of our simulations use a time step of 12 s. Periodic boundary conditions in x and y are imposed at the edges of the domain. To prevent gravity waves reflected at the edges of the domain from propagating back into the vortical area, a simple sponge ring is employed. The sponge ring has a damping coefficient β, which varies radially as shown in Fig. 1, and takes the form of "Rayleigh friction" terms $-\beta(u - \overline{u}_0)$, $-\beta(v - \overline{v}_0)$, and $-\beta(P - \overline{P}_0)$ in the equations of motion for u, v, and P, respectively, where $\overline{u}_0$, $\overline{v}_0$, and $\overline{P}_0$ are the initial azimuthal means of u, v, and P (see above). The maximum damping time $\beta^{-1} \approx 8$ min.

The model also includes fourth-order hyperdiffusion of u, v, and P to remove small-scale effects associated with the enstrophy cascade. A characteristic value of the diffusion coefficient ν_4 is estimated from $\nu_4 \sim (\Delta x)^4/\tau_{\text{eddy}}$, where Δx is the horizontal grid spacing and τ_{eddy} is the eddy turnover time of the vortex defined by

$$\tau_{\text{eddy}} \equiv \frac{2\pi(\text{RMW})}{v_{\max}},$$

where $v_{\max}$ is the basic-state vortex's maximum initial tangential wind speed. Using an RMW of 80 km and a maximum tangential wind of 5 m s^{-1} (see section 3), we obtain $\tau_{\text{eddy}} = 1.0 \times 10^5$ s ≈ 30 h and $\nu_4 = 6.2 \times 10^9$ m^4 s^{-1}. A somewhat smaller value of ν_4 (4.0×10^9 m^4 s^{-1}) was used for the simulations described here. The exponential damping time for grid-scale disturbances is then approximately 40 h. With respect to the vortex-scale features, the results presented here have been verified to be independent of diffuse effects.

b. The nondivergent semispectral model

In addition to the primitive equation model, a semispectral formulation of the nondivergent vorticity equation is used to assess the contributions from wave-mean-flow and wave–wave interactions of vortex Rossby waves in the vortex spinup process.

The nondivergent semispectral model extends the linear numerical model of Montgomery and Kallenbach (1997) to include the nonlinear advective terms (ME, their appendix B). The perturbation streamfunction ψ_S' and the perturbation relative vorticity ζ_S' are represented semispectrally:

$$\psi_S'(r, \lambda, t) = \sum_{l=-N}^{N} \hat{\psi}_l(r, t)e^{il\lambda} \quad \text{and} \tag{1}$$

$$\zeta_S'(r, \lambda, t) = \sum_{m=-N}^{N} \hat{\zeta}_m(r, t)e^{im\lambda}, \tag{2}$$

where an azimuthal wavenumber truncation $N = 16$ is used throughout, "$\hat{}$" denotes azimuthal Fourier amplitude, and the origin is defined at the invariant vorticity centroid. The complete prognostic equation for the streamfunction amplitude is

$$\frac{\partial \hat{\psi}_n}{\partial t} = \nabla_n^{-2}\hat{F}_n(r, t), \tag{3}$$

where

$$\hat{F}_n(r, t) = \frac{1}{r}\Bigg\{ \sum_{\substack{|k|\le N \\ |n-k|\le N}} \left[ik\frac{\partial}{\partial r}(\hat{\psi}_k\hat{\zeta}_{n-k}) - in\hat{\zeta}_{n-k}\frac{\partial \hat{\psi}_k}{\partial r} \right] + in\frac{d\overline{\zeta}}{dr}\hat{\psi}_n - in\frac{d\overline{\psi}}{dr}\hat{\zeta}_n \Bigg\} + \nu\nabla_n^2\hat{\zeta}_n, \tag{4}$$

$\nabla_n^2 = (1/r)\partial/\partial r + \partial^2/\partial r^2 - n^2/r^2$, and bar quantities denote the total azimuthal mean vortex at the previous

time step.[2] A diffusion coefficient ν of 20 m^2 s^{-1} is used in the fully nonlinear simulations to ensure numerical stability at long times.[3] The inversion is carried out using a standard tridiagonal solver. Radial derivatives are computed with centered second-order differences. Time stepping is performed using a standard fourth-order Runge–Kutta scheme. The radial grid spacing is 5 km, with 200 radial points. The time step is 30 s.

In our so-called ''quasilinear'' approximation, products of perturbation quantities in (4) are neglected, and the wavenumber zero basic-state is ''frozen'' in the prediction of the perturbation quantities. The $n \neq 0$ asymmetric modes are thus governed by the inviscid linear Rossby wave equation:

$$\nabla_n^2\left(\frac{\partial\hat{\psi}_n}{\partial t}\right) = in\hat{\psi}_n\frac{\partial\overline{\zeta}}{\partial r} - in\hat{\zeta}_n\frac{\partial\overline{\psi}}{\partial r}. \tag{5}$$

The change in the azimuthal mean tangential wind is then calculated from the change in the pseudo-angular momentum density, or wave activity (Held and Phillips 1987):

$$\delta\overline{v}_t(r, t) = \frac{1}{r}[\overline{A}(r, t) - \overline{A}(r, 0)], \tag{6}$$

where the wave activity $\overline{A}(r, t)$ is defined by

$$\overline{A}(r, t) = \frac{\overline{r\zeta'^2(r, t)}}{2d\overline{\zeta}/dr}, \tag{7}$$

where $\overline{\zeta'^2}$ is the azimuthal mean of the square of the total asymmetric ($n \neq 0$) relative vorticity (perturbation enstrophy), and $d\overline{\zeta}/dr$ the radial derivative of the initial basic-state mean relative vorticity.

In our ''wave-mean-flow'' approximation, the $n \neq 0$ modes still evolve according to (5), but the (azimuthal) mean flow is allowed to change according to

$$\nabla_0^2\frac{\partial\psi_0}{\partial t} = \frac{1}{r}\sum_{|l|\leq N}\left[il\frac{\partial}{\partial r}(\hat{\zeta}_{-l}\hat{\psi}_l)\right]. \tag{8}$$

3. The circular basic-state vortex and the parameterized vorticity and height anomalies

The initial basic-state circular vortex employed here is defined by

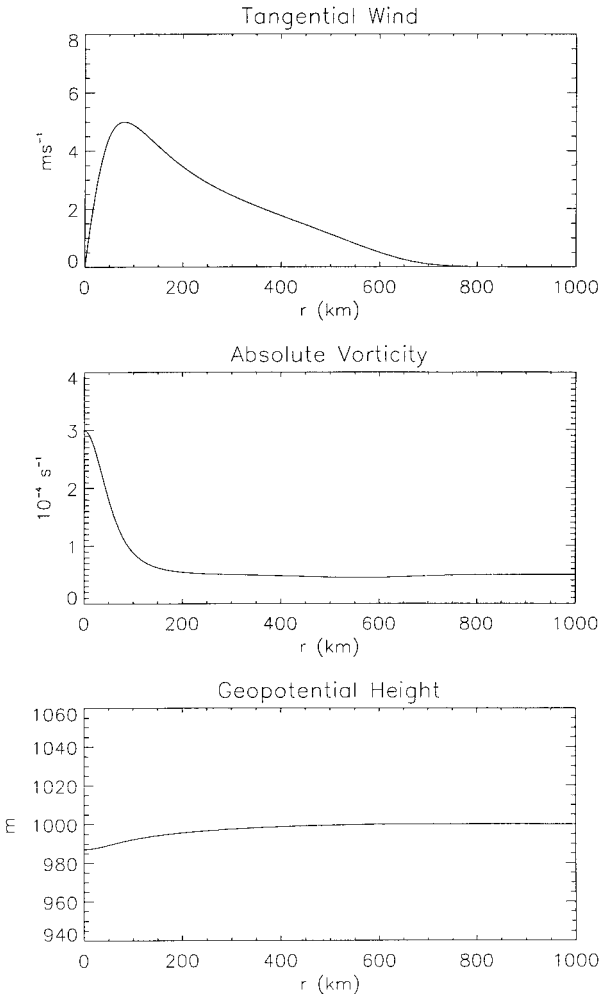

FIG. 2. Initial basic-state tangential wind, absolute vorticity, and geopotential height.

$$\overline{v}_t = 2V_m(r/r_m)\frac{\exp[-a(r/r_m)^b]}{1 + (r/r_m)^2}, \tag{9}$$

where $\overline{v}_t$ is the azimuthal mean tangential wind, r is the radial distance from the center of the vortex, and V_m, r_m, a, and b are constants that define the intensity and radial structure of the vortex (DeMaria 1985). Here the constants are chosen to be appropriate for the tropical cyclogenesis problem (Gray 1998): $V_m = 5$ m s^{-1}, $r_m = 80$ km, $a = 5.5 \times 10^{-6}$, and $b = 6$. The corresponding basic-state circular height field $\overline{h}$ is then deduced from the gradient balance equation:

$$f\overline{v}_t + \frac{\overline{v}_t^2}{r} = g\frac{\partial\overline{h}}{\partial r}. \tag{10}$$

The basic-state tangential wind, vorticity, and geopotential are shown in Fig. 2. Rather than, for example, a Rankine vortex, we have chosen a basic-state vortex with a much broader tangential wind profile, similar to observed tangential wind distributions from aircraft in-

[2] After each time step, the ($l = m = 0$) component of $\{\psi_S', \zeta_S'\}$ generated by wave-mean-flow and wave–wave interactions is added to the previous basic state $\{\overline{\psi}, \overline{\zeta}\}$ to form the updated basic state. The $l = m = 0$ component of (ψ_S', ζ_S') is then zeroed out at the next time step.

[3] The value of ν is sufficiently small here to make a negligible impact on the evolution of the mean vortex and perturbation over timescales of several τ_{eddy}. Virtually identical results are obtained over these timescales on setting $\nu = 0$ in the nonlinear runs of this section.

vestigative flights into convective vortices prior to tropical cyclogenesis (Gray 1998). The effect of the broader vortex is to create a large region of nonzero vorticity gradient on which vortex Rossby waves can propagate, transferring vorticity from convective vorticity anomalies to the mean flow to spin up the initial 5 m s^{-1} vortex (ME).

Rather than explicitly simulate the cloud and mesoscale dynamics for a tropical region (e.g., Weisman et al. 1993; Trier et al. 1996), we take a simple approach and parameterize the vertical vorticity budget of an ensemble of convective cells near an incipient vortex by injecting vorticity anomalies having a horizontal scale of approximately 50–200 km. These vorticity anomalies are chosen to be similar to the convective vorticity anomalies used in ME. The PV magnitudes of the convective anomalies in ME were chosen to be consistent with measured tropical convective heating rates in the generation of lower-tropospheric PV. In this paper our convective vortices have a smaller horizontal scale than those used in the ME simulations, but the magnitude of the vertical vorticity for the anomalies is chosen to give approximately the same cyclonic circulation as the low-level anomalies in ME.

Gentry et al. (1970) reported the low-level convergence field for a large convective asymmetry (called a ''circular exhaust cloud'') derived from aircraft observations of Hurricane Gladys (1968). From their Fig. 10, and assuming a lifetime for a convective blowup during the genesis stage of 6 h, we estimate the total circulation for such a blowup to be approximately 1.9×10^6 m^2 s^{-1}. The total circulation for the single cluster anomaly (see below) used in our simulations is 1.6×10^6 m^2 s^{-1}, in good agreement with the estimate based on the Gentry et al. (1970) data. Thus, in addition to the estimate of ME, the result based on the Gentry et al. (1970) data gives us further confidence that our convective anomaly magnitudes are realistic.

For our simulations we assume that convection occurs in one, two, or four regions or ''clusters.'' These cases are termed the single-, double-, and four-cluster anomalies, respectively. The double-cluster anomaly is given by

$$\zeta_2' = \zeta_{\max}' \begin{cases} \sin^2\left[\dfrac{\pi(\delta r_1 - \Delta)}{2\Delta}\right] & \text{if } \delta r_1 \le \Delta; \\ \sin^2\left[\dfrac{\pi(\delta r_2 - \Delta)}{2\Delta}\right] & \text{if } \delta r_2 \le \Delta; \\ 0, & \text{otherwise.} \end{cases} \tag{11}$$

Here δr_1 and δr_2 are the distances from the anomaly centers (x_{c1}, y_{c1}) and (x_{c2}, y_{c2}): $\delta r_1 = [(x - x_{c1})^2 + (y - y_{c1})^2]^{1/2}$ and $\delta r_2 = [(x - x_{c2})^2 + (y - y_{c2})^2]^{1/2}$, and ζ'_{max} and Δ are parameters describing the amplitude and width of the anomaly, respectively. The values of x_{c1}, x_{c2}, y_{c1}, y_{c2}, ζ'_{max}, and Δ are listed in Table 1. The initial condition $\zeta = \zeta_2' + \zeta_{\rm bs}$, where ζ is the total vorticity and $\zeta_{\rm bs}$ is the vorticity of the DeMaria basic state, is shown in Fig. 3a.

TABLE 1. Parameters describing the primitive equation PV anomalies.

Parameter	Value
x_{c1}	1100 km
x_{c2}	900 km
y_{c1}	1000 km
y_{c2}	1000 km
$\zeta_{\max}$	1.74×10^{-4} s^{-1}
Δ	100 km
x_{d1}	1050 km
x_{d2}	1100 km
x_{d3}	1150 km
x_{d4}	1100 km
y_{d1}	1000 km
y_{d2}	950 km
y_{d3}	1000 km
y_{d4}	1050 km
$\zeta_{4,\max}$	1.74×10^{-4} s^{-1}
Δ_4	50 km

The single-cluster anomaly is given by

$$\zeta_1' = \zeta_{\max}' \begin{cases} \sin^2\left[\dfrac{\pi(\delta r_1 - \Delta)}{2\Delta}\right] & \text{if } \delta r_1 \le \Delta; \\ 0, & \text{otherwise.} \end{cases} \tag{12}$$

This initial condition is shown in Fig. 3b.

Finally, since observations show that convection is often not confined to a single cluster, but has a more patchy distribution, we used a four-cluster initial condition as shown in Fig. 3c. The four-cluster initial condition is designed to have the same cyclonic circulation as the single cluster. The four-cluster initial condition is given by

$$\zeta_4' = \zeta_{4,\max}' \sum_{\substack{i=1,4 \\ \delta\tilde{r}_i < \Delta_4}} \sin^2\left[\frac{\pi(\delta\tilde{r}_i - \Delta_4)}{2\Delta_4}\right]. \tag{13}$$

Here $\delta\tilde{r}_1$, $\delta\tilde{r}_2$, $\delta\tilde{r}_3$, and $\delta\tilde{r}_4$ are the distances from the anomaly centers (x_{d1}, y_{d1}), (x_{d2}, y_{d2}), (x_{d3}, y_{d3}), and (x_{d4}, y_{d4}), respectively. The x and y values of the anomaly centers Δ_4 and $\zeta'_{4,\max}$ are listed in Table 1.

For each of the anomaly configurations, a small correction is added to the wind field at each point in the model domain to ensure that the anomalous vorticity integrated over the entire computational domain is zero; that is, we enforce zero circulation on the anomalies. In the quasigeostrophic model this was done more naturally based on the integral constraints.

Initialization for the shallow water model proceeds as follows. First, initial values of the basic state u and v at each grid point are generated using Eq. (9). The vorticity field given by Eqs. (11), (12), or (13) is then defined at each grid point, and successive overrelaxation is applied to calculate ψ', the anomaly streamfunction, from

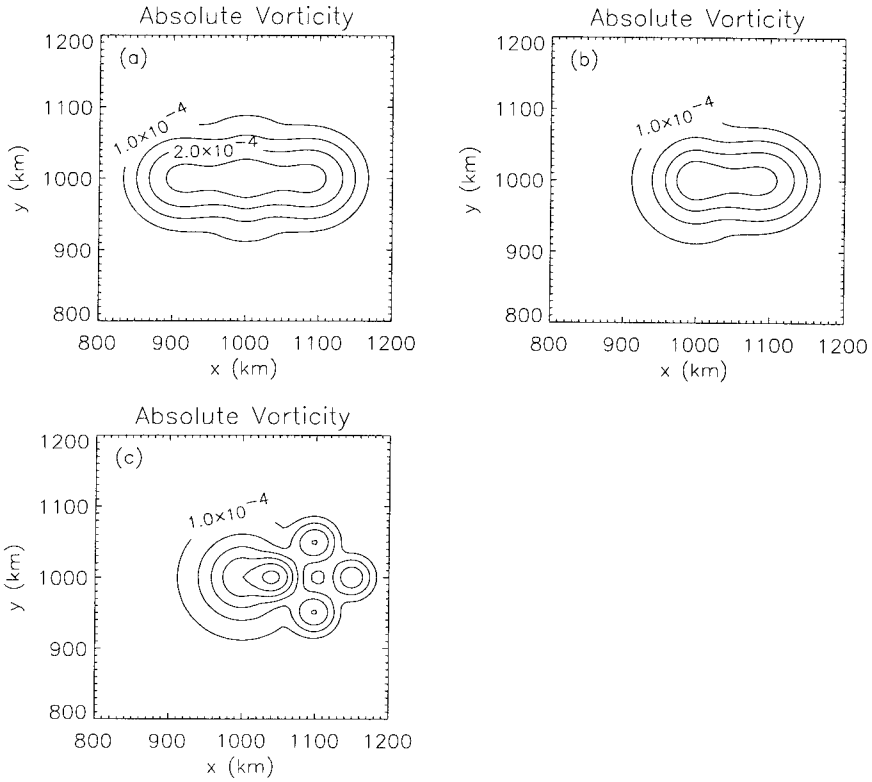

FIG. 3. Initial total absolute vorticity for (a) the double-cluster configuration, (b) the single-cluster configuration, and (c) the four-cluster configuration. Only the inner 400 km × 400 km of the model domain are shown. Contour interval is 5×10^{-5} s^{-1}.

$$\nabla^2\psi' = \zeta'. \tag{14}$$

Here u' and v' are then calculated via $\mathbf{Z} \times \nabla\psi'$, where $\mathbf{Z}$ is the vertical unit vector, and added to the basic-state winds. Finally, in cases for which a balanced height field is desired, a successive overrelaxation for

$$\nabla^2 P = \left[f\zeta + 2\left(\frac{\partial v}{\partial y}\frac{\partial u}{\partial x} - \frac{\partial v}{\partial x}\frac{\partial u}{\partial y}\right)\right] \tag{15}$$

is performed to calculate the height field in nonlinear balance (Holton 1992; McWilliams 1985) with the total wind field (basic state + anomalies). The tolerance required for the streamfunction is $(\nabla^2\psi' - \zeta')_{\max} < 10^{-7}$ s^{-1} (i.e., the maximum residual is less than 1/500 of the planetary vorticity), while the tolerance required for the height field is $\{\nabla^2 P - (f\zeta + 2[(\partial v/\partial y)(\partial u/\partial x) - (\partial v/\partial x)(\partial u/\partial y)])\}_{\max} < 10^{-11}$ s^{-2} (i.e., the maximum residual is less than 1/500 of $f\zeta \approx 5 \times 10^{-9}$). Solutions for ψ' and P are accurate to approximately 1%.

4. Comparison with previous quasigeostrophic results

In this section we compare the cyclogenesis results obtained with the primitive equation model to the results obtained previously with a quasigeostrophic model (ME). Montgomery and Enagonio (1998) found a spin-up of 1 m s^{-1} for double-cluster anomalies associated with a 200-km RMW basic-state vortex with 5 m s^{-1} maximum tangential wind. For the primitive equation model, which permits arbitrary values of the Rossby number and unbalanced initial data, we use a balanced vortex that also has 5 m s^{-1} maximum mean tangential wind but has an 80-km RMW, more closely matching the typical dimensions of mesoscale convectively generated vortices (Bartels and Maddox 1991). The convective anomalies (see section 3) have a more compact structure than the Gaussian anomalies used in ME; however, the maximum vorticity of the new anomalies was chosen so that the total cyclonic circulation of the convective anomalies is approximately equal to that of the low-level double-cluster anomalies in ME's quasigeostrophic model. To begin, the ''basic state + anomaly'' initial fields are assumed to be in nonlinear balance. This assumption will be relaxed shortly.

The time evolution of the vorticity field for the double-cluster experiment is shown in Fig. 4a. The initial and final azimuthal mean tangential winds $\overline{v}_t$ and the change in $\overline{v}_t$ for the double-cluster experiment in the primitive equation model are shown in Fig. 5. Note that, although the basic-state state vortex has 5 m s^{-1} maximum wind, the initial azimuthal mean tangential wind in Fig. 5 is approximately 7.4 m s^{-1}, due to the contribution from the wavenumber zero component of the

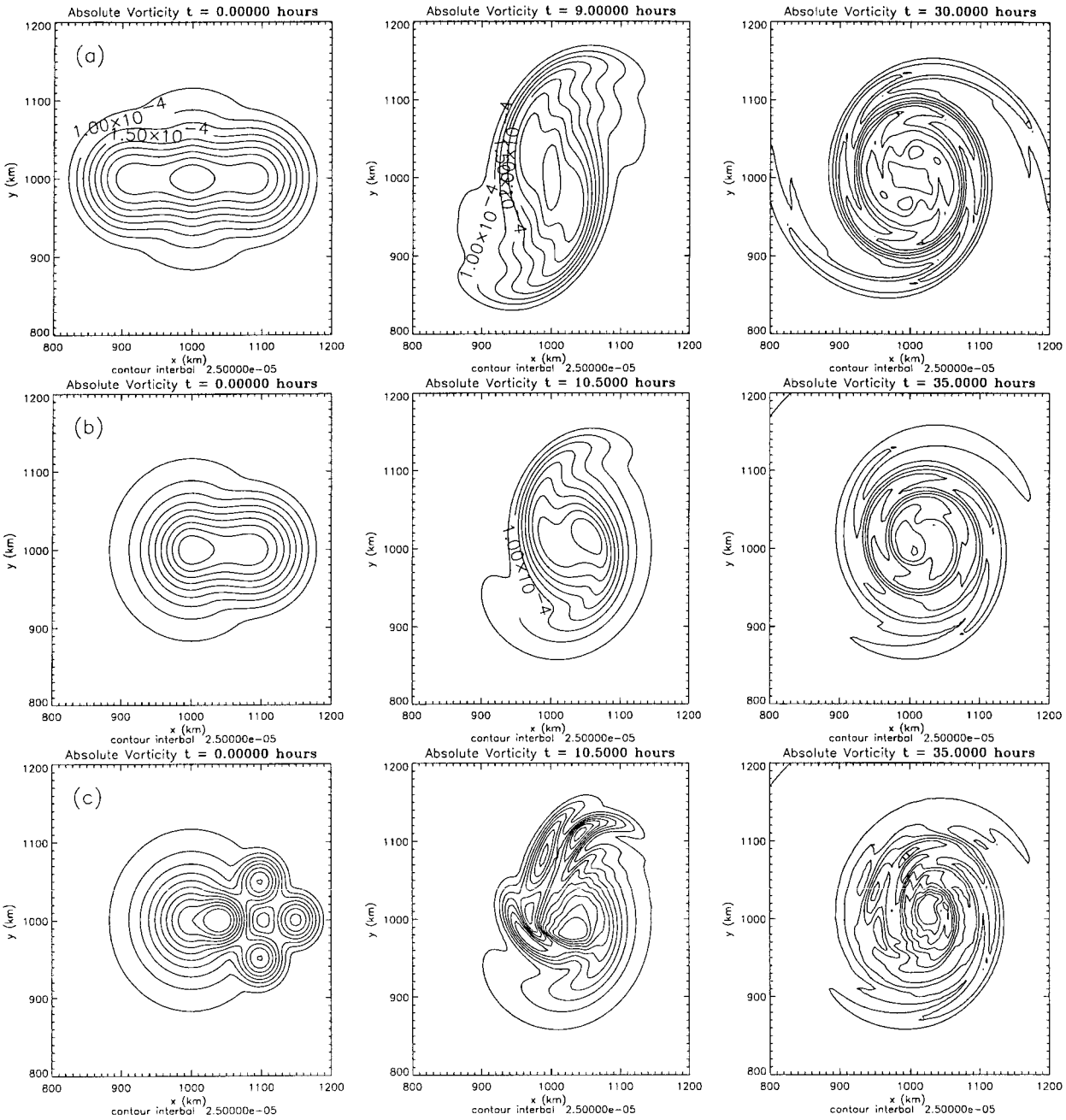

FIG. 4. Time evolution of the absolute vorticity field for (a) basic state + nominal double-cluster anomaly; (b) basic state plus nominal single-cluster anomaly; (c) basic state plus four-cluster anomaly. Only the innermost 400 km × 400 km of the model domain is shown.

convective anomalies. Figure 5 shows a net spinup, shape, and location—near the RMW—very similar to the results obtained in the quasigeostrophic model (cf. Fig. 9b in ME). The change in vorticity, shown in Fig. 5 is also qualitatively similar to the quasigeostrophic result shown in Fig. 9a of ME, but of larger magnitude due to the smaller horizontal scale of the initial anomalies.

An experiment with a single convective cluster was also performed and compared to the quasigeostrophic results. Again the maximum vorticity of the anomaly in the primitive equation model was chosen to give approximately the same total cyclonic circulation as the low-level single-cluster anomaly in the quasigeostrophic studies. The time evolution of the vorticity field for the single-cluster experiment is shown in Fig. 4b. The change in mean tangential wind and in vorticity over a time period sufficient for axisymmetrization are shown in Fig. 6. These plots are again similar to the quasigeostrophic predictions of ME (their Fig. 10b). We note

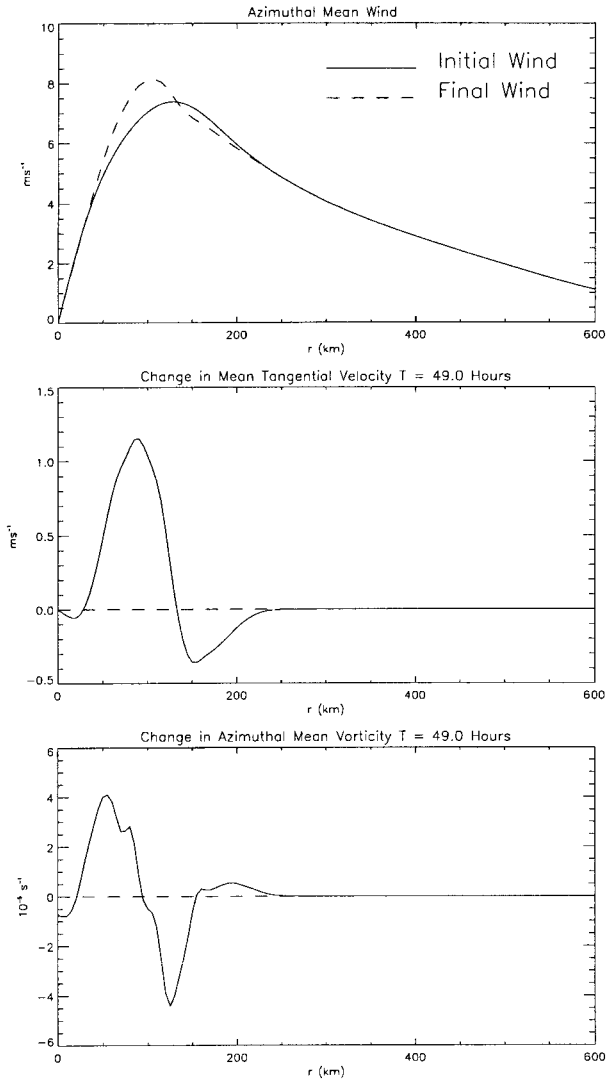

FIG. 5. Azimuthal mean tangential wind $\overline{v}_t$ at $T = 0$ and $T = 49$ h ($1.6\tau_{\text{eddy}}$), change in azimuthal wind $\delta\overline{v}_t$ over the 49-h period, and change in vorticity $\delta\overline{\zeta}$ over 49 h for the double-cluster convective experiment. Only the innermost 600 km of the model domain is shown.

that, although for the double-cluster experiment the wavenumber zero component of the anomaly has a rather large projection of 2.4 m s^{-1} on the initial 5 m s^{-1} basic-state vortex, the single-cluster case has a significantly weaker (1.5 m s^{-1}) projection onto the initial basic state.

The maximum change in mean tangential velocity is plotted as a function of integration time in Fig. 7a for double cluster and in Fig. 7b for single cluster. The quasigeostrophic results are shown for comparison. In these plots the integration time is expressed in units of the eddy turnover time defined in section 2. In calculating τ_{eddy} we use the RMW of the total azimuthal mean vortex (basic-state vortex plus the wavenumber zero component of the convective anomalies). It is evident from Fig. 7 that the vortex spinup exhibits an approximately universal behavior versus t/τ_{eddy}. Thus one concludes that for the smaller incipient vortices used here spinup will occur faster than for the quasigeostrophic experiments of ME, for which spinup times of order 3 days were predicted. In section 5 we demonstrate that with a succession of convective episodes we obtain spinup of a 15 m s^{-1} vortex in approximately 40 h. If the convective anomalies were stronger or—as demonstrated in section 5—if the convective outbreaks were nearer to the center of the basic-state vortex, we could obtain spinup to a tropical storm in less than 30 h.

It should be noted that the total spinup for the quasigeostrophic single-cluster case reported here is 0.5 m s^{-1}, rather than the value of 0.4 m s^{-1} reported in ME. Here we report results in the zero-diffusive limit (rather than the weakly diffusive limit) for comparison with the primitive equation results that are obtained with biharmonic diffusion. Our previous results underestimated the quasigeostrophic single-cluster spinup by about 20%. This is a small error compared to the uncertainty in the amount of vertical vorticity generated by the convective outbreaks.

The reader may inquire as to the relationship between the results discussed here and the extensive body of literature on two-dimensional vortex merger alluded to in the introduction to this paper. Examination of the vorticity fields produced in our experiments shows that, because of the small distance between the vortices, in all cases we have examples of the case of ''complete merger'' described by Dritschel and Waugh (1992). That is, the final resultant configuration consists of a single central vortex including fluid from each of the original vortices, as well as surrounding filaments (see Fig. 4). What is new in our work is the description of vortex merger in terms of such basic state vortex plus vorticity anomaly interactions, including the relationship of the magnitudes of the vortices and spinup times to realistic physical parameters. Moreover, the use of the quasilinear and wave-mean-flow approximations discussed in section 5 for the purpose of assessing the degree of nonlinearity in such vortex interactions is also new and insightful. In addition, ME examined the eddy-forced secondary circulation that attends these interactions and elucidated the formation of the cyclone's warm core as a natural by-product of three-dimensional axisymmetrization.

It is now of interest to consider initial conditions for which the wind field and the height field are not in balance. Figure 8 shows the evolution of the height field at early times for initial conditions having vorticity given by Eq. (11) but no height anomaly; that is, the height field is only that of the circular basic-state vortex given by Eqs. (9) and (10). The initially circular height field is quickly deformed to an elliptical state, and early in the experiment the cross-section plots show the excitation of gravity waves, identified by their rapid propagation out of the vortical region. Here $\delta\overline{v}_t$ and $\delta\overline{\zeta}$ for this case, compared to the case of balanced initial con-

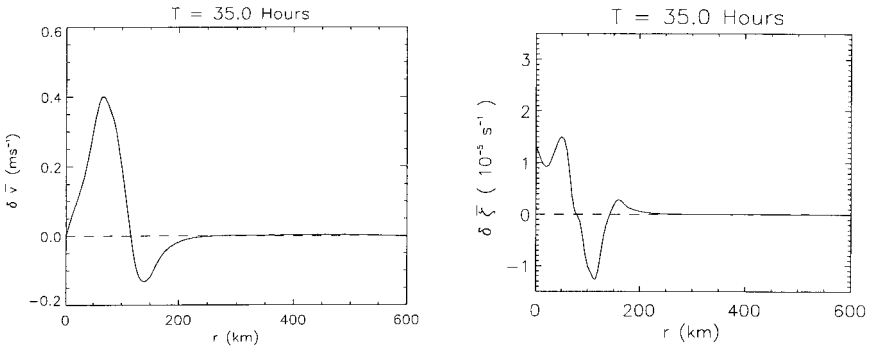

FIG. 6. Change in the azimuthal mean tangential wind and azimuthal mean vorticity over $1.3\tau_{\text{eddy}}$ for the single-cluster convective experiment. Only the innermost 600 km of the model domain is shown.

ditions, are shown in Fig. 9. The shapes are very similar to those of the balanced double-cluster experiment. The magnitude of the spinup is only slightly less than for the balanced case, implying that only a small fraction of the available kinetic energy associated with the vorticity anomaly is carried away by gravity waves. Figure 10 shows the maximum increase in mean tangential velocity versus integration time for the wind anomaly only case. The spinup time is also quite similar to that for the balanced case, which is to be expected since the gravity wave adjustment is observed to occur rapidly compared to the the vortex spinup, as indicated by Fig. 10. The gravity wave adjustment timescale τ_a is given approximately by the inverse of the effective Coriolis parameter for the axisymmetric vortex (Schubert et al. 1980; Shapiro and Montgomery 1993),

$$\tau_a \approx \frac{1}{\left[\left(f + \frac{2\overline{v}_t}{r}\right)(f + \overline{\zeta}_r)\right]^{1/2}} \approx 1.7 \text{ h}.$$

Here $\overline{\zeta}_r$ is the azimuthal mean relative vorticity for our vortex at the radial position (100 km) of the anomalies; based on the results shown in Figs. 7 and 10 the axisymmetrization time is on the order of two to three times the shear time τ_s at that radius, where

$$\tau_s = \left[r\frac{d(\overline{v}_t/r)}{dr}\right]^{-1} \approx 6.9 \text{ h} \quad \text{at radius 100 km}.$$

We are aware of the fact that ''axisymmetrization'' does not always go to completion within several τ_s because of excitation of near-discrete (quasi-mode), discrete neutral, or unstable vortex Rossby waves in association with wave-induced changes to the mean potential vorticity [see, e.g., ME and Möller and Montgomery (1999) for examples and discussion; see also Schecter et al. (2000) and Balmforth et al. (2000, and references therein)]. The ''spinup'' ideas advanced here are nevertheless believed to remain approximately valid for near-core vorticity anomalies in regions where the radical mean PV gradient is sufficiently large (see section 5a). The fact that the gavity wave adjustment time is significantly less than the axisymmetrization time (scale separation) is consistent with our expectations based on τ_a and τ_s. As long as $\tau_a < \tau_s$, we expect the upgradient vorticity transport mechanism by linear (and nonlinear) vortex Rossby waves to be unimpeded by gravity waves (see section 5b).

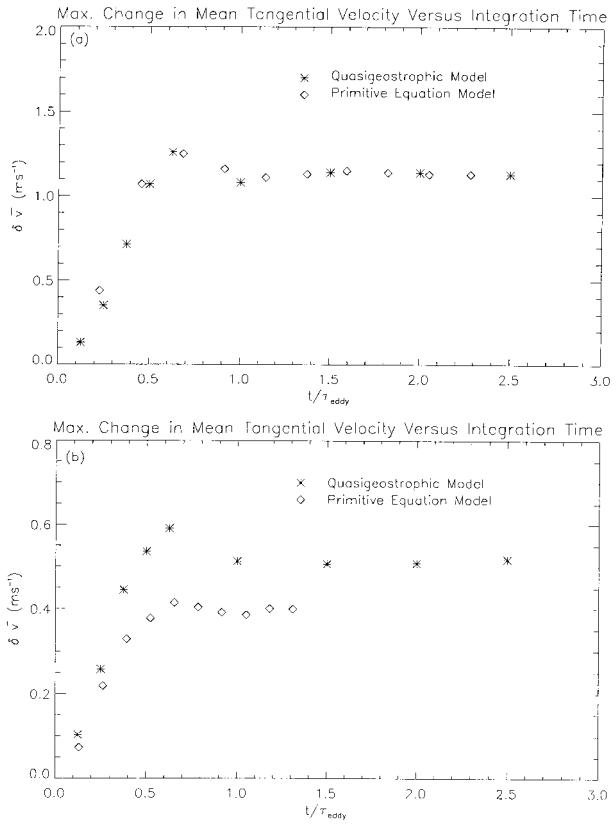

FIG. 7. Maximum change in azimuthal mean tangential wind as a function of integration time for (a) the double-cluster experiment and (b) the single-cluster experiment. The quasigeostrophic results are shown in the no-diffusion limit.

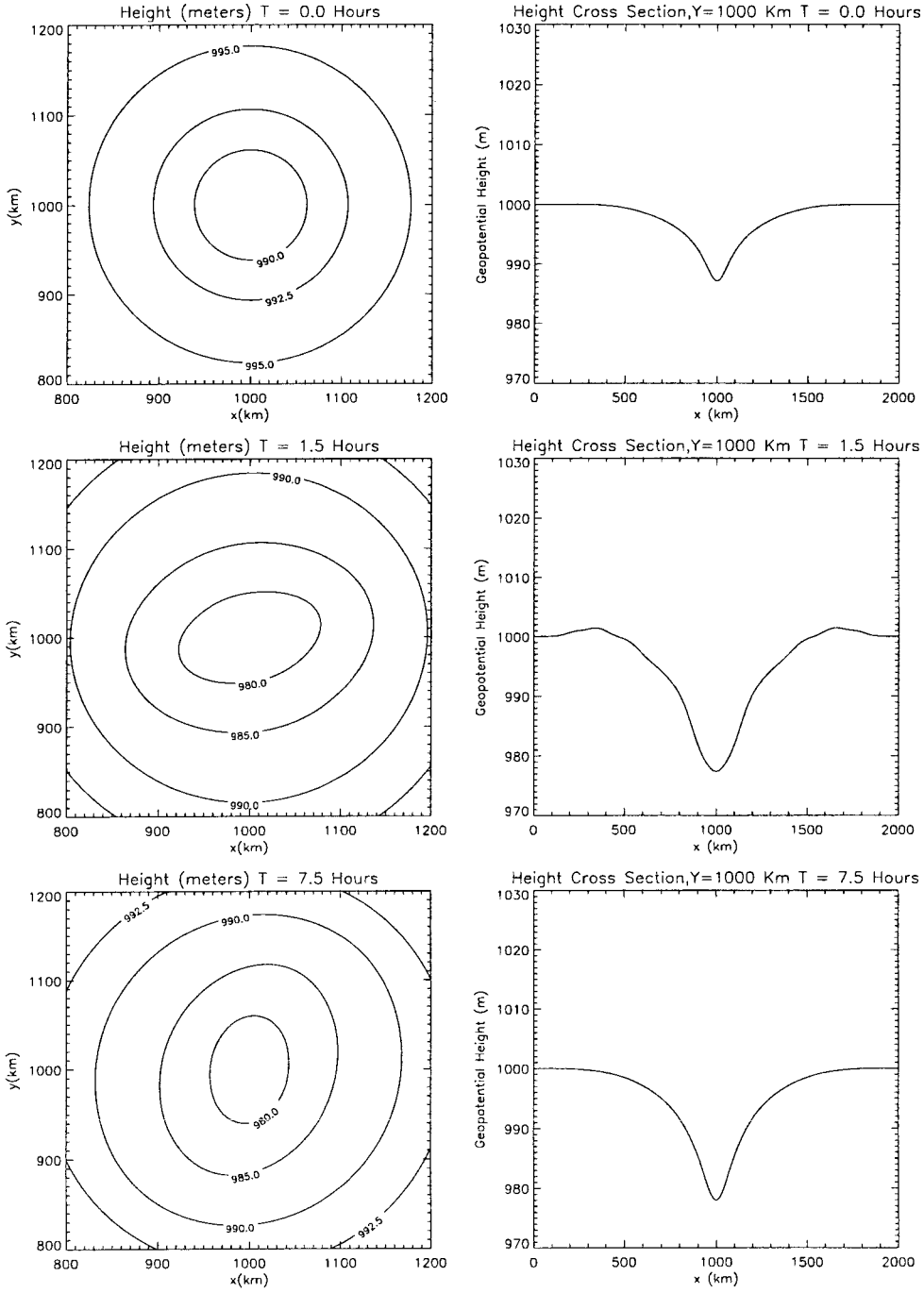

FIG. 8. Contours of free-surface height and cross section of height along $y = 1000$ km for $T = 0$, 1.5, and 7.5 h for the double-cluster experiment with no anomaly in the height field. Note that only subsets of the total model domain are shown.

We also performed an experiment with the double-cluster anomaly, but with the anomaly appearing only in the height field (no anomalous winds). In contrast to the case of the wind field anomaly, the height field anomaly run showed very little spinup. For this case $\delta\overline{v}_t$ and $\delta\overline{\zeta}$ are also shown in Fig. 9.

The results for the experiments with unbalanced and nonaxisymmetric initial conditions are to be expected qualitatively on the basis of the axisymmetric calculations of Schubert et al. (1980) using a nonresting basic-state vortex as well as the seminal works of Rossby (1937) and Obukhov (1949). For convectively generated

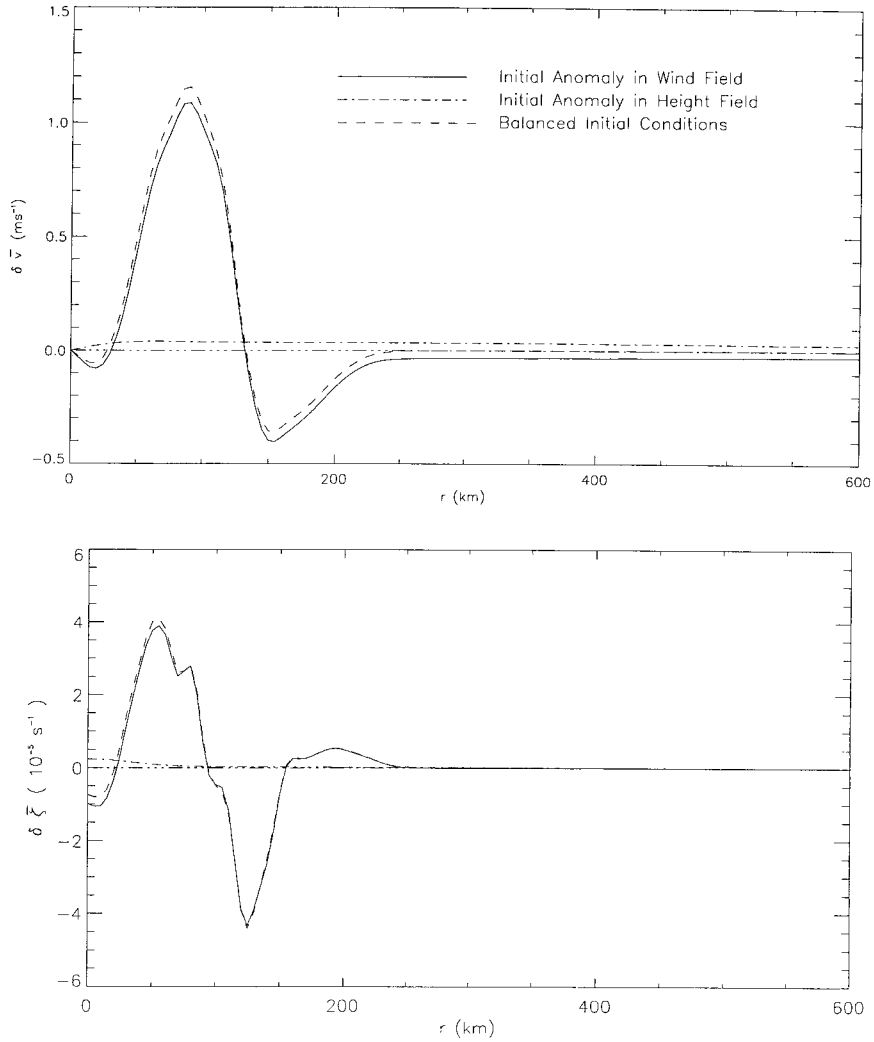

FIG. 9. Comparison of the change in the azimuthal mean tangential wind and change in the azimuthal mean vorticity for the double-cluster convective experiments with anomaly only in the wind field, only in the height field, and balanced anomaly. Only the innermost 600 km of the model domain is shown.

disturbances whose horizontal scales are small compared to the (local) Rossby radius of deformation ($\simeq$600 km near the core for the weak vortices employed here), the energy of nonaxisymmetric rotational disturbances appears mostly in the final balanced flow, and thus contributes to spinning up the tangential wind of the mean vortex. The energy of disturbances to the mass (height) field appears mostly in gravity–inertia waves, which propagate rapidly out of the vortical region and are eventually damped by the sponge ring.

A comparison between the primitive equation double-cluster results and the corresponding calculation in a nondivergent simulation is shown in Fig. 11. The excellent agreement between the primitive equation and nondivergent simulations is to be expected because the Froude number in our primitive equation experiments is much less than one (McWilliams 1985).

5. Further results with the primitive equation model

a. Vorticity anomalies of varying amplitude

Thus far we have considered the interaction of basic-state and convective vortices for which the convective vortex is of comparable amplitude (in vorticity) to the basic-state vortex. We now consider the behavior of such systems when the convective vortex becomes significantly stronger than the basic-state vortex. This issue for general vortices has previously been investigated by Melander et al. (1987b). One might expect that in this case

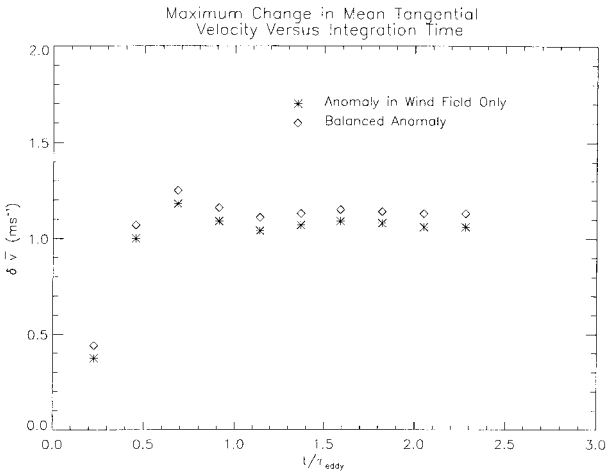

FIG. 10. Maximum change in azimuthal mean tangential wind as a function of integration time for the double-cluster convective experiment with the convective anomaly in the wind field only. The double-cluster experiment with balanced initial conditions is shown for comparison.

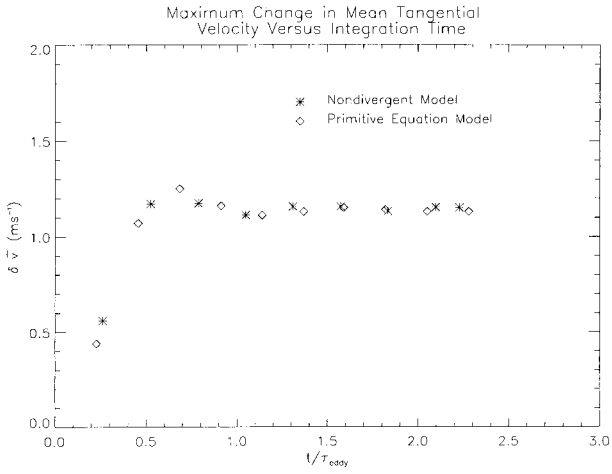

FIG. 11. Maximum change in azimuthal mean tangential wind as a function of integration time for the primitive equation model compared to the corresponding nondivergent calculation.

the strong convective vortex becomes the dominant member of the pair, advecting and shearing the basic-state vortex. Figure 12 shows the evolution of the vorticity fields for the nominal basic state and single-cluster anomaly strength (Fig. 12a), and for two other cases having the same basic-state vortex but the vorticity amplitude of the single-cluster anomaly increased by a factor of 2 (Fig. 12b) and then by a factor of 4 (Fig. 12c). In each case the area of the cyclonic vorticity anomaly has been adjusted to keep the cyclonic circulation of the anomaly invariant. For the case of the 4× nominal strength anomaly, the convective vortex does indeed become the dominant vortex, shearing and advecting the basic-state vortex around itself while retaining its own basic structure until an approximately axisymmetric configuration is obtained. In the case of the nominal-strength anomaly, the basic state is dominant, shearing and advecting the convective anomaly, so that the final configuration is again approximately axisymmetric. For the 2× nominal strength anomaly, an intermediate behavior is observed, with both vortices shearing and advecting each other until near axisymmetrization is obtained.

A heuristic criterion for determining whether the convective vorticity anomaly disperses on a smooth and monotonically decreasing basic-state vorticity distribution in the core region can be deduced on examining the ratio of the nonlinear terms in the vorticity equation to the linear vortex Rossby wave (restoring) term, that is, the *vortex beta Rossby number* R_β, which scales as

$$R_\beta \sim \frac{v'_{\rm rms}}{L^2 \dfrac{d\bar{\zeta}}{dr}},$$

where v'_{rms} is a characteristic root-mean-square eddy velocity for eddy scale L, and $d\bar{\zeta}/dr$ is the azimuthal mean radial vorticity gradient of the basic-state vortex.[4] Use of a beta Rossby number is familiar from work examining the motion of an intense vortex on a beta plane (McWilliams and Flierl 1979; Reznik and Dewar 1994; Montgomery et al. 1999). The beta Rossby number is introduced here simply to quantify the relative importance of linear vortex Rossby wave processes to nonlinear processes at early times. When a circular vortex is placed on a beta plane the analogous ratio is

$$R_\beta^{\rm motion} \sim \frac{\bar{v}}{({\rm RMW})^2 \beta},$$

where $\bar{v}$ is the vortex's maximum mean tangential wind and β is df/dy. In the beta-plane problem the vortex is regarded as the eddy, whereas for the tropical cyclogenesis problem the convective anomaly is regarded as the eddy. Thus in both cases the large beta Rossby number corresponds to the eddy remaining intact with weak Rossby wave dispersion, while the small beta Rossby number corresponds to the eddy dissipating through strong Rossby wave dispersion and shearing in the vortex case. Further use of the vortex beta Rossby number and its dependence on the Rossby deformation radius is considered in Möller and Montgomery (2000) and RM.

The values of R_β for the nominal, 2× nominal, and 4× nominal cases are found to be approximately 0.3, 0.8, and 2.4 at the center of the vorticity anomalies, respectively (see Table 2). Thus we expect the intermediate wave-mean-flow approximation to capture the essence of the anomaly–vortex interaction in the relax-

[4] These experiments at large amplitude are performed with the SWPE model.

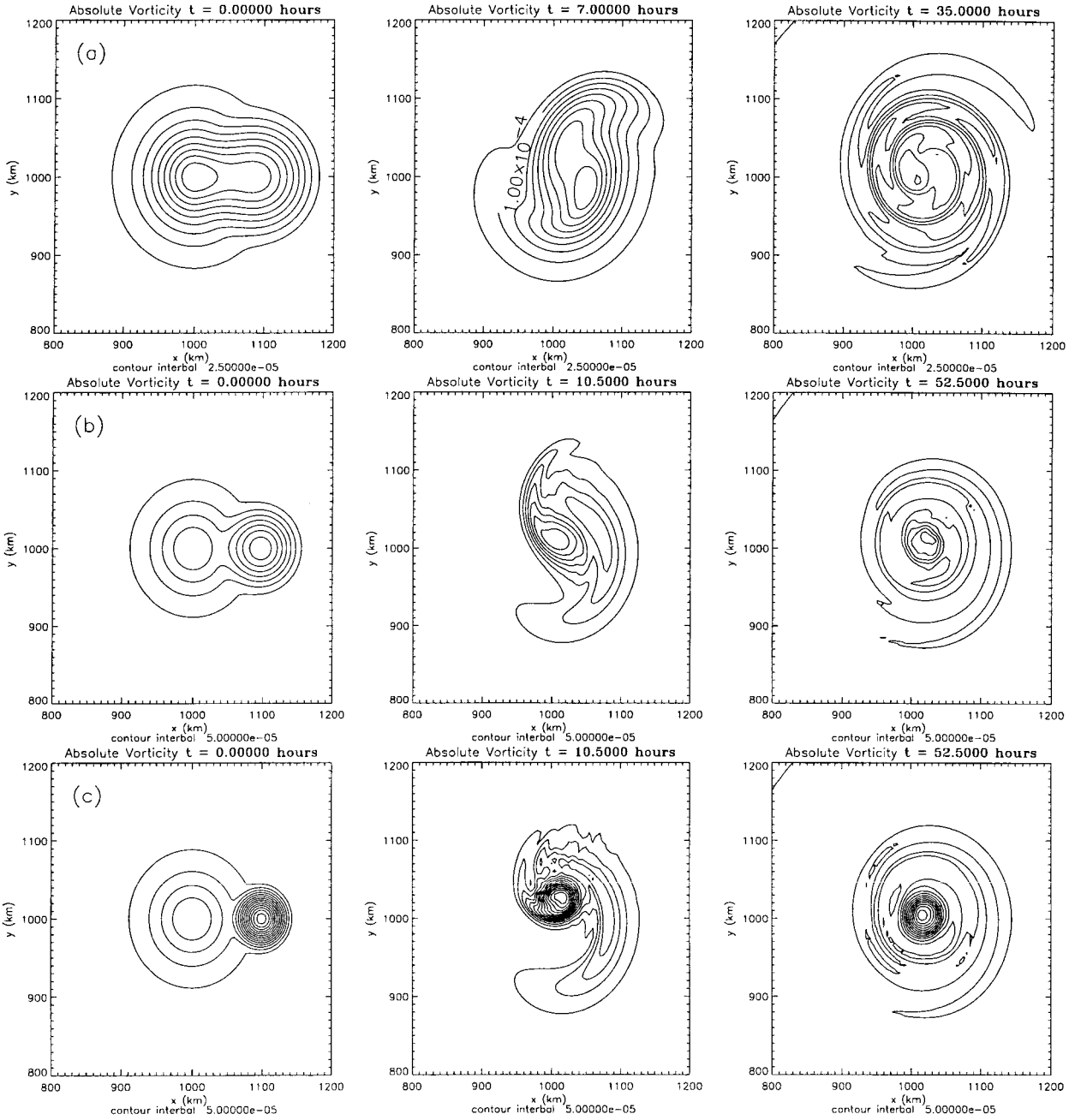

FIG. 12. Time evolution of the absolute vorticity field for (a) basic state + nominal single-cluster anomaly, (b) basic state plus 2× nominal single-cluster anomaly, and (c) basic state plus 4× nominal single-cluster anomaly. Only the innermost 400 km × 400 km of the model domain is shown.

ation experiments for the nominal amplitude case but not for the other cases. The results of Fig. 12 are consistent with this picture.[5]

For the 4× nominal case, it is of interest to calculate R_β considering the convective anomaly as the ''basic state'' and the DeMaria vortex as the ''eddy.'' Taking

[5] *Note added in proof:* For large-amplitude vorticity anomolies ($R_\beta \gg 1$) whose circulation is small compared to the ''master'' vortex an analytical theory has been developed recently by Schecter and Dubin (1999). This approach appears useful when large-amplitude small-scale vorticity anomalies are generated in tropical cyclones. Cloud-resolving simulations now offer the opportunity to test these theories.

TABLE 2. Vortex beta Rossby numbers for configurations with vortices of varying amplitudes and spatial scales.

Configuration	R_β
Nominal single cluster	0.3
Single cluster, 2× nominal amplitude	0.8
Single cluster, 4× nominal amplitude	2.4
DeMaria vortex considered as eddy	0.08

$v'_{\rm rms} = 5$ m s^{-1}, $L = 70$ km, and $d\overline{\zeta}/dr$ for the convective anomaly to be 1.3×10^{-8} m^{-1} s^{-1}, we obtain $R_{\beta,\rm DeMaria} = 0.08$. Thus we expect the wave-mean-flow picture to be approximately valid for the DeMaria vortex considered as the eddy, explaining why the DeMaria vortex is dispersed by the convective anomaly. The initial and final azimuthal mean tangential winds about the center of the convective anomaly (actually the geopotential minimum for the domain, which approximately coincides with the center of the convective anomaly) and $\delta\overline{v}_t$ are shown in Fig. 13. A broadening of the $\overline{v}_t$ profile is observed, but the maximum $\overline{v}_t$ does not change significantly.

b. Further relaxation experiments

Sometimes the convection surrounding an incipient tropical cyclone has a patchy appearance, rather than occurring in a single mass such as our single-cluster convective anomaly. To simulate this effect, we performed an experiment with the four-cluster anomaly described in section 3. The four-cluster simulation could not be performed in ME because the decrease in cluster radius implies an effective Rossby number Ro of order unity. For the four-cluster anomaly the Rossby number is

$$\text{Ro} \approx \frac{3 \text{ m s}^{-1}}{(5 \times 10^{-5} \text{ s}^{-1})(50 \times 10^{3} \text{ m})} = 1.2.$$

Figure 14 shows $\delta\overline{v}_t$ and $\delta\overline{\zeta}$ for this case as simulated in the SWPE, for a balanced initial condition model. Since circulation is the parameter in our simplified model measuring the strength of the convective anomalies, for purposes of comparison the four-cluster anomaly is defined so that its net cyclonic circulation is equal to that of the single-cluster anomaly. The four-cluster case gives a maximum $\delta\overline{v}_t$, which is approximately half that of the single-cluster case (cf. Fig. 6). The basic axisymmetrization process, shown in Fig. 4c looks quite similar, as does the shape of the $\delta\overline{v}_t$ plot (Fig. 14), indicating that the fundamental spinup mechanism is unchanged.

Although the reason for the smaller spinup in the four-cluster case, as opposed to the single-cluster case, is not yet fully understood, we have been able to reproduce this effect, first discovered in our primitive equation model, in the nondivergent semispectral model. Figure 15 shows the primitive equation results compared to the fully nonlinear nondivergent model results. It is seen that the fully nonlinear nondivergent model reproduces

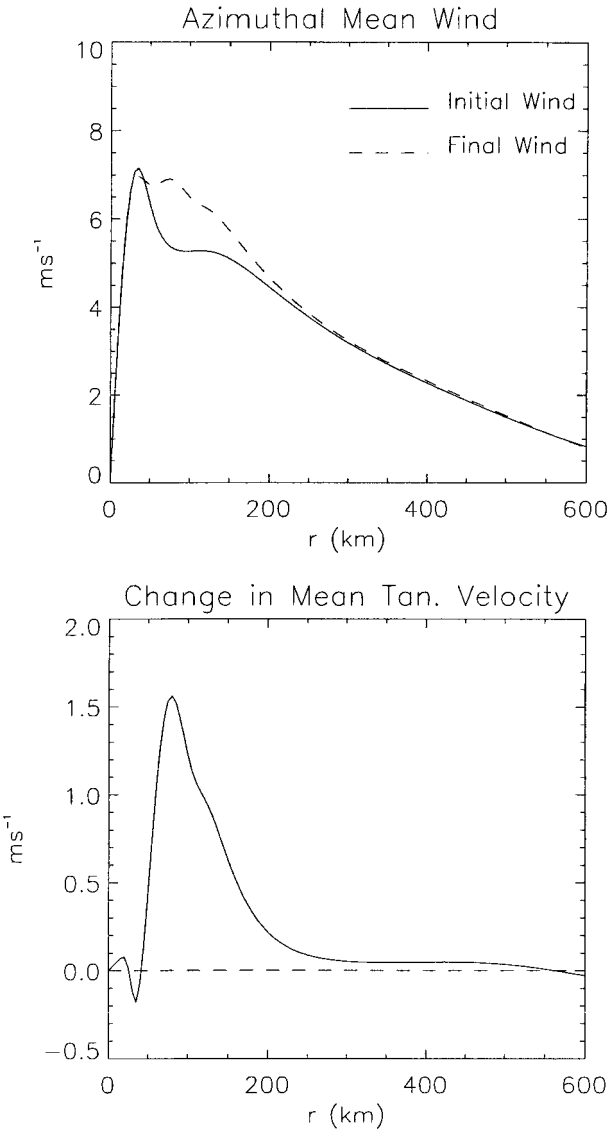

FIG. 13. Azimuthal mean tangential wind $\overline{v}_t$ at $T = 0$ and $T = 35$ h and change in azimuthal wind $\delta\overline{v}_t$ over the 35-h period about the center of the convective anomaly. Only the innermost 600 km of the model domain is shown.

the effect of less spinup in the four-cluster than in the single-cluster case. This is not surprising considering Fig. 9. More remarkable perhaps is that the wave-mean-flow approximation, which only allows the 16 azimuthal modes to interact with the wavenumber zero mean flow, gives a good approximation of the primitive equation results, even at these large amplitudes. The results of the wave-mean-flow simulations are also shown in Fig. 15. The R_β values for the single-cluster and four-cluster configurations are estimated to be approximately 0.3 and 1.2, respectively, explaining the efficacy of the wave-mean-flow approximation at reproducing the fully nonlinear results for these configurations. The quasilinear nondivergent simulation (not shown) does not, however,

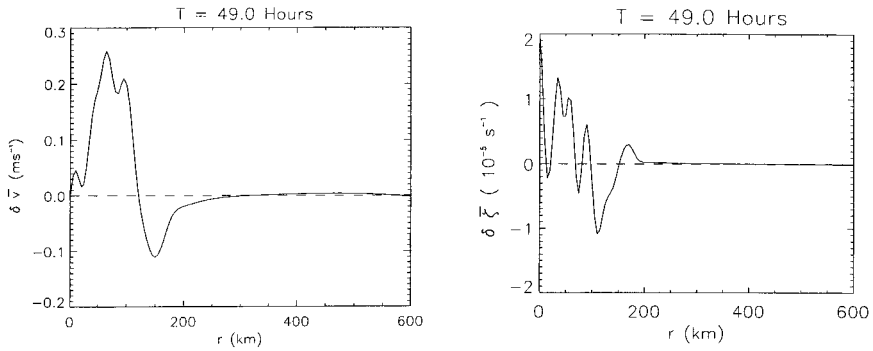

FIG. 14. Change in the azimuthal mean tangential wind and azimuthal mean vorticity over $1.6\tau_{\text{eddy}}$ for the four-cluster convective experiment (Fig. 4c). Only the innermost 600 km of the model domain is shown.

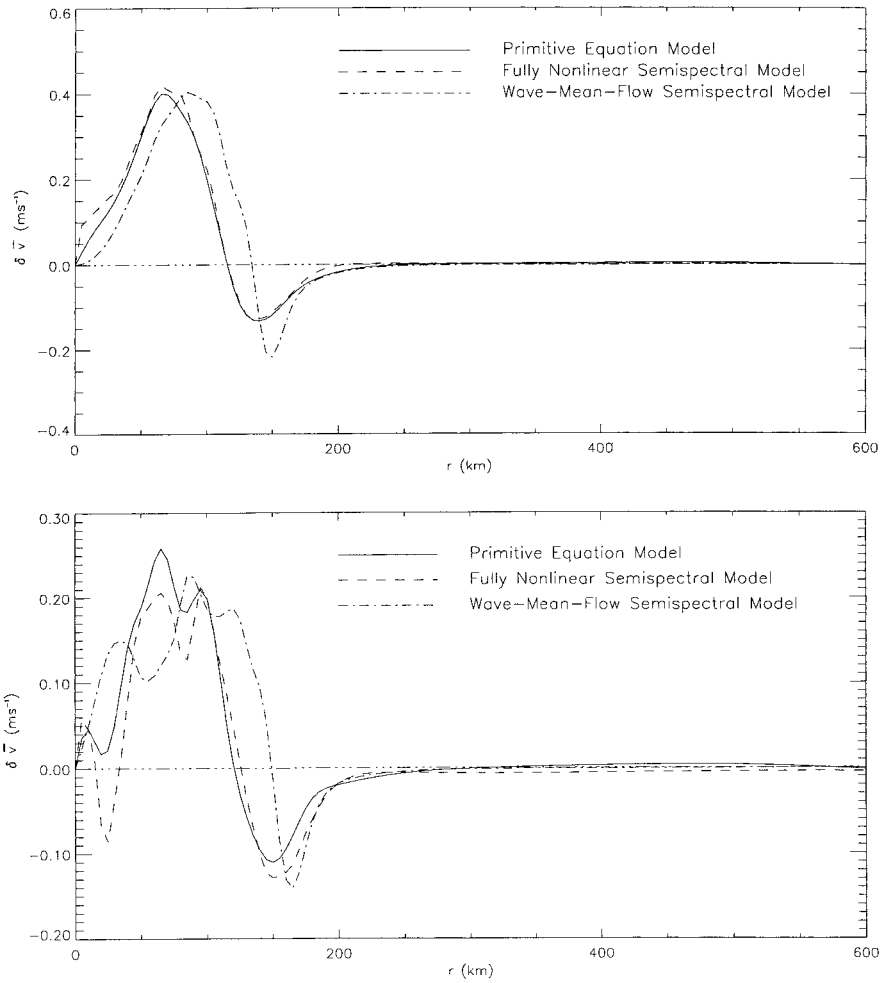

FIG. 15. Change in the azimuthal mean tangential wind for the single-cluster and four-cluster convective experiments in the primitive equation model (Figs. 4b and 4c, respectively) compared to the same results in the semispectral fully nonlinear and wave-mean-flow simulations. Only the innermost 600 km of the model domain is shown.

reproduce the difference between the four-cluster and single-cluster configurations, with the maximum $\delta\overline{v}_t$ for the two configurations being approximately the same in the quasilinear simulations and a factor of 2 too large.

The quantitative disagreement between the ''quasi-linear'' and ''wave-mean-flow'' prediction is not surprising in light of the large-amplitude vorticity anomalies employed. But the reasonably close agreement in the mean flow change between the wave-mean-flow model and the fully nonlinear model deserves brief comment. By Stokes' theorem the strengthening of the mean tangential wind implies a radially inward (upgradient) transport of like-sign eddy vorticity. The wave-mean-flow predictions of Fig. 15 show that the bulk of this inward transport is produced by *linear* vortex Rossby waves. Vortex merger via linear vortex Rossby waves for small but finite amplitude vorticity anomalies near or within the RMW of a smoothly distributed vortex was first predicted by Montgomery and Kallenbach (1997, their section 2h). The results of Fig. 15 provide confirmation of the robustness of their prediction for large-amplitude vorticity anomalies [provided R_β is $\leq 0(1)$]. Lagrangian trajectory calculations in both ''quasi-linear'' and ''wave-mean-flow'' models (not shown here) further illustrate the predicted effect and demonstrate the ingestion of like-sign eddy vorticity inside the RMW and expulsion of like-sign and opposite-sign eddy vorticity into vortex filaments that orbit the vortex core.[6]

c. Pulsing experiments

Thus far we have considered relaxation experiments, in which an initial basic-state vortex and PV anomaly are allowed to axisymmetrize. Similar to ME we next consider the case of ongoing convection over a several-day period, by adding ''pulses'' of convection periodically (normally every $0.5\tau_{\text{eddy}}$, which for our basic-state vortex corresponds to a frequency of approximately 15 h). This approach allows us to emulate the multiple bursts of convection observed by Zehr (1992), and also shown in Fig. 16 of ME. Although the pulses of convection shown in the figure have a duration of approximately 6 h, this feature is difficult to simulate in the primitive equation model; rather, our pulses consist of an input of vorticity shaped just like the initial convective anomalies at the chosen time step in the model. *The pulse anomalies are in the wind field, with no anomaly in the height field, so that the pulses are far out of balance.* Unlike the quasigeostrophic simulations of ME, we did not find it necessary to allow the pulse amplitude to grow during each simulation; rather, all pulses for a given simulation have the same amplitude. The pulsed experiments, similar to those of ME, are here performed in the SWPE model to verify that unbalanced dynamics give similar results to those of balanced dynamics in the quasigeostrophic model.

Figure 16a shows the mean tangential wind of the main vortex at initial and final times for a pulsed simulation. The simulation consists of an initial pulse of convection at $T = 0$ with four additional convective pulses spaced evenly throughout the run. The tangential wind increases through the simulation, spinning up from 6 m s^{-1} to 15 m s^{-1} in the course of the model run. Thus, with realistic magnitudes for the convective anomalies, the model predicts spinup to near-tropical storm strength in 75 h.

We have also investigated the effect of doubling the convective pulse frequency, and have obtained spinup to a 15 m s^{-1} vortex in approximately 40 h. The mean tangential wind at initial and final times for this ''high-frequency'' case is shown in Fig. 16b. It should be noted that the estimate of the magnitude of the convective anomalies made in ME is conservative, so we consider the scenario of spinup from a 5 m s^{-1} vortex to a tropical storm in 40 h by the suggested mechanism to be quite plausible. If convection occurs near the center of the initial vortex (see following paragraph), or the maximum cyclonic vorticity is larger than used here, the spinup process would occur even more rapidly. We also performed a simulation in which the initial basic-state vortex had a RMW of 50 km rather than the 80-km nominal value; results with the 50-km vortex are shown in Fig. 16c. The spinup for this case is similar to the other pulsed experiments; actually, it is somewhat stronger.

As was the case in the quasigeostrophic simulations, the achieved spinup is rather sensitive to the radial location of the convective pulses. Table 3 shows the maximum $\delta\overline{v}_t$ and maximum final tangential wind as the location of the multiple convective pulses is varied from radius $r = 0$ to 200 km. For the larger radii, spinup occurs outside the initial RMW and thus the final maximum azimuthal mean tangential winds are lower than for the cases with convection closer to the center of the vortex. This effect is also to be expected based on the

[6] *Note added in proof:* Lagrangian trajectories induced by purely *linear* dynamics are presented in section 4 of RM.

→

FIG. 16. (a) Azimuthal mean tangential wind at initial and final times for a pulsed single-cluster simulation. Only the innermost 600 km of the model domain is shown. (b) Azimuthal mean tangential wind at initial and final times for a high-frequency pulsed single-cluster simulation. Spinup to a greater than 15 m s^{-1} vortex is obtained in less than 40 h. Only the innermost 600 km of the model domain is shown. (c) Azimuthal mean tangential wind at initial and final times for a pulsed single-cluster simulation with the basic-state vortex having an initial radius maximum wind of 50 km rather than the nominal 80 km. Only the innermost 600 km of the model domain is shown.

(a)

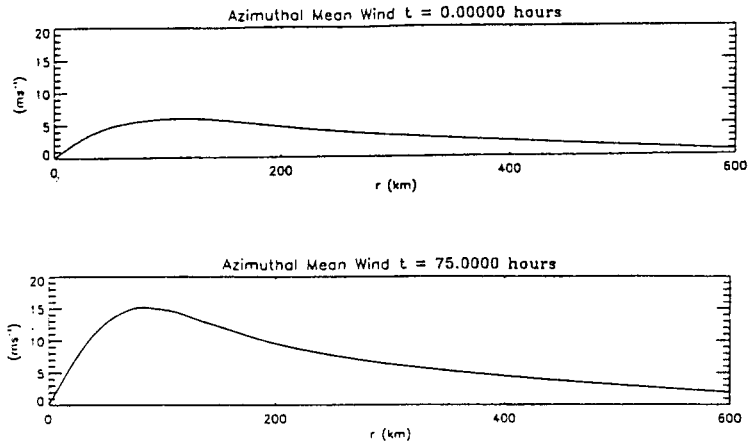
Azimuthal Mean Wind t = 0.00000 hours
(ms⁻¹)
r (km)
Azimuthal Mean Wind t = 75.0000 hours
(ms⁻¹)
r (km)

(b)

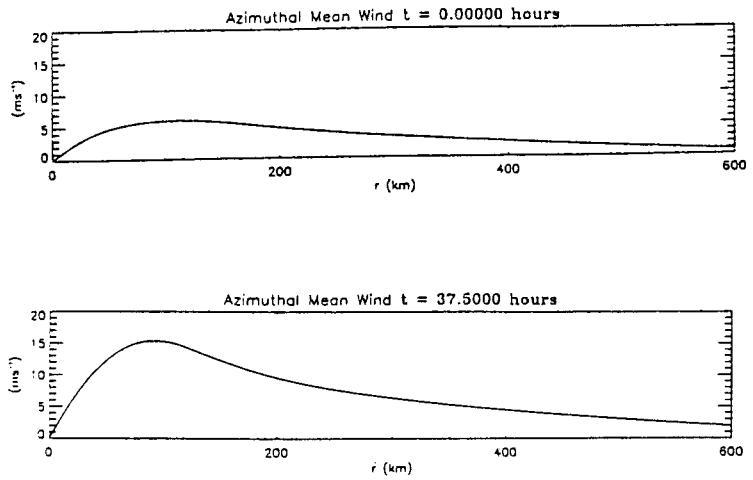
Azimuthal Mean Wind t = 0.00000 hours
(ms⁻¹)
r (km)
Azimuthal Mean Wind t = 37.5000 hours
(ms⁻¹)
r (km)

(c)

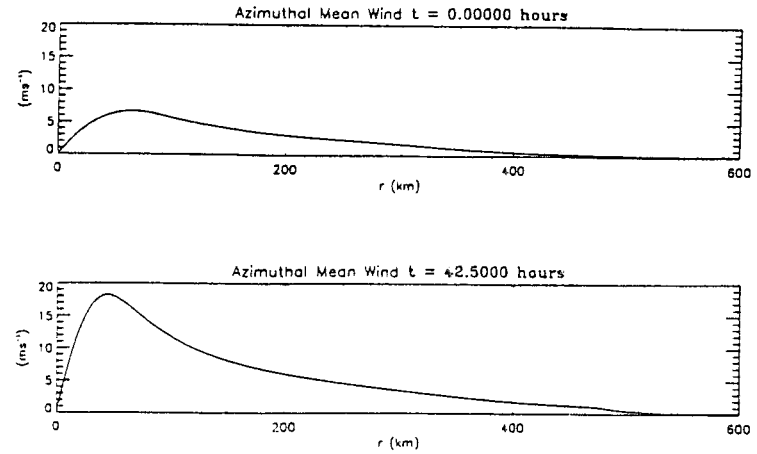
Azimuthal Mean Wind t = 0.00000 hours
(ms⁻¹)
r (km)
Azimuthal Mean Wind t = 42.5000 hours
(ms⁻¹)
r (km)

TABLE 3. Final maximum azimuthal mean tangential wind and maximum change in the azimuthal mean tangential wind as a function of the radial location of the convective cluster from the initial vortex center for pulsed experiments.

Radius of convective anomaly (km)	$\overline{v}_{t,\max}$ (m s^{-1})	$\delta\overline{v}_t$ (m s^{-1})
0	20.7	12.6
100	15.2	9.5
160	12.0	7.2
200	10.2	5.8

observations described in Gray (1998) and Lunney (1988), in which greater magnitude radial winds and more deep convection occur within the inner 2° radius for developing genesis cases as compared to nondevelopers. Our model results also predict a broader tangential wind profile when the convective asymmetries occur relatively far outside the RMW.

The largest increase in tangential velocity occurs when the convective pulses are placed at the center of the initial basic-state vortex (as also found by ME). The reader may thus wonder why our emphasis is on the importance of asymmetries in the spinup process. Assuming that at the genesis stage the preexisting vortex does not strongly organize the convection, it is more probable that convective outbreaks will occur distributed over the vortex's area rather than very close to the center. The observations by Lee (1986, 1989a,b) also indicate that asymmetries comprise the largest contribution to the tangential momentum budget during genesis. When convective outbreaks very near the center of the incipient vortex do occur, they can be expected to generate stronger and more rapid spinup than when the asymmetries are at the RMW or even farther from the incipient vortex's center.

We also tested the sensitivity of the spinup to the *x*–*y* orientation of the pulses, with a model run of what we called ''scrambled'' pulses. In this run, the initial single-cluster convective anomaly is located, as for the nominal single-cluster experiment, at a radius of 100 km from the center of the basic-state vortex along the *x* axis. However, the first secondary pulse anomaly is placed at 100-km radius along the *y* axis, rotated 90° from the initial anomaly. The second secondary pulse is rotated back 90° to the position of the initial anomaly, and thereafter the pulses alternate between these two orientations along the *x* and *y* axes. The scrambled pulse run gives similar results to the nominal single-cluster run, with a final maximum azimuthal mean tangential velocity of 13.4 m s^{-1}, as compared to 15.2 m s^{-1} for the nominal 100-km radius single-cluster pulsed simulation. Thus our results are not strongly sensitive to the *x*–*y* orientation of the pulses.

The results for the single-cluster pulsed experiments are displayed in Table 4.

TABLE 4. Sensitivity tests of the shallow water primitive equation model under pulsed convective forcing.

Run type	Maximum $\delta\overline{v}_t$ (m s^{-1})
Nominal single cluster with control basic state	9.5
Nominal single cluster with control basic state, high frequency	9.5
Scrambled single cluster with control basic state	7.4
Single cluster with 50-km RMW	12.2

6. Recent satellite observations of convective asymmetries

Suggestions of tropical cyclone intensification due to convective asymmetries or ''blowups'' are frequently visible in satellite IR imagery. Here we present a case study taken from Geostationary Meteorological Satellite data. The vortex in this example is already of tropical storm strength, so this is not a case of genesis, but rather of intensification; a tropical storm was chosen so that the main vortex could be easily identified from IR imagery. We nevertheless believe that the example is suggestive of the way that convective blowups may contribute to spinup at the genesis stage.

Figure 17 shows a time sequence of IR images for Tropical Cyclone Todd in September 1998. The first image shows the cloud patterns at 0425 UTC on 16 September. Summary information for this storm indicates that Todd had an estimated maximum 10-min sustained near-surface wind speed of 18 m s^{-1} at 0000 UTC and 23 m s^{-1} at 0600 UTC. At 0425 UTC the vortex appears quite symmetric and minimum IR temperatures are between −80°C and −90°C. In the second image, taken at O630 UTC, an asymmetric outbreak of convection on the east side of the vortex is seen, with minimum IR temperatures less than −90°C. In the next image, at 0830 UTC, the convective asymmetry appears to have been advected around the storm's circulation center. By the fourth image, at 1025 UTC, the convective asymmetry has apparently merged with the storm, so that the asymmetry is no longer clearly distinguishable. In the fifth image, at 1130 UTC, the storm again shows an approximately symmetric shape, with the near-surface wind estimated at 31 m s^{-1} near that time. These observations are suggestive of an outbreak of deep convection near an approximately symmetric vortex, with the convective asymmetry merging (axisymmetrizing) with the main storm vortex on a timescale of 4–5 h, and resultant spinup of the storm from 18–23 m s^{-1} to 31 m s^{-1} during that time. This storm intensified very rapidly, with near-surface winds increasing from 23 m s^{-1} to 59 m s^{-1} in just 18 h, corresponding to a pressure drop using Dvorak's table of 64 mb per 18 h (J. Knaff 1999, personal communication).

7. Summary and conclusions

The results of ME for tropical cyclogenesis via convectively forced vortex Rossby waves in balanced qua-

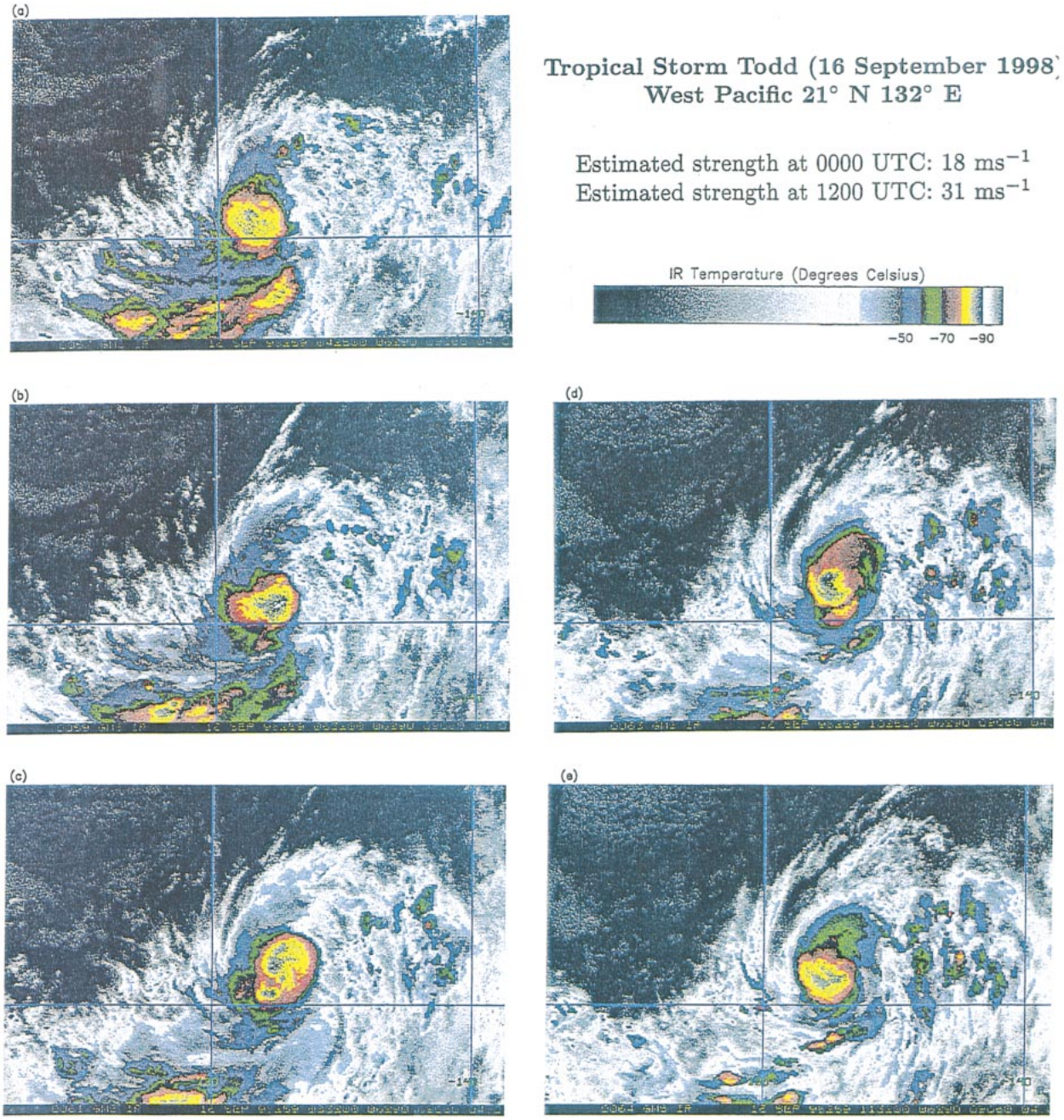

FIG. 17. IR imagery for tropical cyclone Todd on 16 Sep 1998. Blue, green, red, yellow, and white areas indicate −50°, −60°, −70°, −80°, and −90°C contours, respectively: (a) 0425, (b) 0630, (c) 0830, (d) 1025, and (e) 1130 UTC.

sigeostrophic framework have been validated in a shallow water primitive equation framework. The three-dimensional quasigeostrophic predictions for the spinup time and magnitude of an initial 5 m s^{-1} basic-state vortex forced by convective vorticity anomalies have been compared with primitive equation results. Spinup magnitudes are comparable and spinup times are found to be an approximately universal function of t/τ_{eddy}. An important consequence of this latter result is that spinup in smaller basic-state vortices is more rapid than in the quasigeostrophic simulations. With episodic convective forcing we obtain spinup to a tropical storm strength vortex in approximately 40 h. Fully nonlinear simulations with the semispectral model are in good agreement with the primitive equation model. For initial conditions in which the wind and mass fields are not in balance, we obtain comparable magnitudes of spinup to that obtained in the balanced case provided that the initial forc-

ing is in the vortical field rather than the mass (height) field. Although the latter is to be expected based on simple geostrophic adjustment ideas and nonacceleration theorems generalized to an isolated vortex in gradient balance (Schubert 1985; MK, section 4; Montgomery and Lu 1997; cf. Kuo and Polvani 1999) these experiments succinctly demonstrate this point for asymmetric disturbances.

We have addressed the issue of what will occur when a convective vorticity anomaly is substantially stronger than the 5 m s^{-1} basic-state vortex. In this case the convective anomaly becomes the dominant or master vortex, remaining essentially intact and shearing the basic-state vortex with resultant spinup of the convective anomaly. This behavior is explained heuristically in terms of a vortex beta Rossby number, which provides a local estimate of the initial relative magnitudes of the nonlinear terms in the vorticity equation to the linear Rossby wave restoring term.

Additional numerical simulations show that, when convection occurs in multiple patches or clusters with equal circulation, the spinup of the initial basic-state vortex is significantly decreased. This effect is also observed in experiments with a nondivergent semispectral model. A wave-mean-flow approximation also captures the reduction of vortex spinup occurring with multiple-cluster convection. The usefulness of the wave-mean-flow approximation at the relatively large amplitudes considered here is explained by the fact that, due to the large vorticity gradients of these basic-state vortices, the vortex beta Rossby numbers are not large.

A case study using satellite observations suggests intensification of a tropical storm by asymmetric deep convection. Similar results for earlier times in the lifecycle of a tropical cyclone would be of great interest. Further observational tests of our theory require finescale vorticity maps in the region of tropical disturbances, which do or do not develop into tropical cyclones. Observations of the shearing of convective vorticity patches, upgradient and downgradient vorticity transport would be of interest. Work is under way to test the ideas presented here in a ''full-physics'' context using mesoscale numerical models, such as RAMS and MM5. The results will be reported in due course.

Acknowledgments. This work was supported in part by National Science Foundation Grant NSF 9732678 and Colorado State University. We gratefully acknowledge the contribution of Dr. John Knaff of the Cooperative Institute for Research in the Atmosphere at Colorado State University, who provided us with the satellite pictures used in section 6. We also thank Dr. Wayne Schubert for drawing to our attention some of the early literature on convective asymmetries in tropical cyclones.

REFERENCES

Balmforth, N. J., S. G. Llewellyn-Smith, and W. R. Young, 2000, Disturbing vortices. *J. Fluid Mech.*, in press.

Bartels, D. L., and R. A. Maddox, 1991: Midlevel cyclonic vortices generated by mesoscale convective systems. *Mon. Wea. Rev.*, **119,** 104–117.

Bassom, A. P., and A. D. Gilbert, 1998: The spiral wind-up of vorticity in an inviscid palnar vortex. *J. Fluid Mech.*, **371,** 109–140.

——, and ——, 1999: The spiral wind-up and dissipation of vorticity and a passive scalar in a strained planar vortex. *J. Fluid Mech.*, **398,** 245–270.

Black, P. G., F. D. Marks Jr., and R. A. Black, 1986: Supercell structure in tropical cyclones. Preprints, *Joint Sessions 23d Conf. on Radar Meteorology and Conf. on Cloud Physics*, Vol. 3, Snowmass, CO, Amer. Meteor. Soc., JP255–JP259.

Carr, L. E., III, and R. T. Williams, 1989: Barotropic vortex stability to perturbations from axisymmetry. *J. Atmos. Sci.*, **46,** 3177–3191.

DeMaria, M., 1985: Tropical cyclone motion in a nondivergent barotropic model. *Mon. Wea. Rev.*, **113,** 1199–1210.

Dritschel, D. G., and D. W. Waugh, 1992: Quantification of the inelastic interaction of unequal vortices in two-dimensional vortex dynamics. *Phys. Fluids A,* **4,** 1737–1744.

Enagonio, J., and M. T. Montgomery, 1998: Tropical cyclogenesis via convectively forced vortex Rossby waves in a three-dimensional quasigeostrophic model. Paper 656, Dept. of Atmospheric Science, Colorado State University, 115 pp. [Available from Dr. Michael T. Montgomery, Department of Atmospheric Science, Colorado State University, Fort Collins, CO 80523-1371.]

Gamache, J. F., R. A. Houze Jr., and F. D. Marks Jr., 1993: Dual-aircraft investigation of the inner core of Hurricane Norbert. Part III: Water budget. *J. Atmos. Sci.*, **50,** 3221–3243.

Gentry, R. C., T. T. Fujita, and R. C. Sheets, 1970: Aircraft, spacecraft, satellite and radar observations of Hurricane Gladys, 1968. *J. Appl. Meteor.*, **9,** 837–850.

Gray, W. M., 1968: Global view of the origin of tropical disturbances and storms. *Mon. Wea. Rev.*, **96,** 669–700.

——, 1998: The formation of tropical cyclones. *Meteor. Atmos. Phys.*, **67,** 37–69.

Guinn, T. A., and W. H. Schubert, 1993: Hurricane spiral bands. *J. Atmos. Sci.*, **50,** 3380–3403.

Held, L. M., and P. J. Phillips, 1987: Linear and nonlinear barotropic decay on the sphere. *J. Atmos. Sci.*, **44,** 200–207.

Holland, G. J., and G. S. Dietachmayer, 1993: On the interaction of tropical-cyclone-scale vortices. III: Continuous barotropic vortices. *Quart. J. Roy. Meteor. Soc.*, **119,** 1381–1398.

Holton, J. R., 1992: *An Introduction to Dynamic Meteorology.* 3d ed. Academic Press, 511 pp.

Kuo, A. C., and L. M. Polvani, 1999: Wave-vortex interactions in rotating shallow water. Part 1. One space dimension. *J. Fluid. Mech.*, **394,** 1–27.

Lansky, I. M., T. M. O'Neil, and D. A. Schecter, 1997: A thoery of vortex merger. *Phys. Rev. Lett.*, **79,** 1479–1482.

Lee, C. S., 1986: An observational study of tropical cloud cluster evolution and cyclogenesis in the western North Pacific. Paper 403, Dept. of Atmospheric Science, Colorado State University, 250 pp. [Available from Department of Atmospheric Science Research Library, Colorado State University, Fort Collins, CO 80523-1371.]

——, 1989a: Observational analysis of tropical cyclogenesis in the western North Pacific. Part I: Structural evolution of cloud clusters. *J. Atmos. Sci.*, **46,** 2580–2598.

——, 1989b: Observational analysis of tropical cyclogenesis in the western North Pacific. Part II: Budget analysis. *J. Atmos. Sci.*, **46,** 2599–2616.

Lunney, P. A., 1988: Environmental and convective influences on tropical cyclone development vs. nondevelopment. Paper 436, Dept. of Atmospheric Science, Colorado State University, 105 pp. [Available from Department of Atmospheric Science Research Library, Colorado State University, Fort Collins, CO 80523-1371.]

Marks, F. D., Jr., R. A. Houze Jr., and J. F. Gamache, 1992: Dual-

aircraft investigation of the inner core of Hurricane Norbert. Part I: Kinematic structure. *J. Atmos. Sci.,* **49,** 919–942.

McCalpin, J. D., 1987: On the adjustment of azimuthally perturbed vortices. *J. Geophys. Res.,* **92,** 8213–8225.

McWilliams, J. C., 1985: A uniformly valid model spanning the regimes of geostrophic and isotropic, stratified turbulence: Balanced turbulence. *J. Atmos. Sci.,* **42,** 1773–1774.

——, and G. R. Flierl, 1979: On the evolution of isolated, nonlinear vortices. *J. Phys. Oceanogr.,* **9,** 1155–1182.

Melander, M. V., J. C. McWilliams, and N. J. Zabusky, 1987a: Axisymmetrization and vorticity-gradient intensification of an isolated two-dimensional vortex through filamentation. *J. Fluid Mech.,* **178,** 137–159.

——, N. J. Zabusky, and J. C. McWilliams, 1987b: Asymmetric vortex merger in two dimensions: Which vortex is ''victorious''? *Phys. Fluids,* **30,** 2610–2612.

——, ——, and ——, 1988: Symmetric vortex merger in two dimensions: Causes and conditions. *J. Fluid Mech.,* **195,** 303–340.

Molinari, J., P. Moore, and V. Idone, 1999: Convective structure of hurricanes as revealed by lightning locations. *Mon. Wea. Rev.,* **127,** 520–534.

Möller, J. D., and M. T. Montgomery, 1999: Vortex Rossby waves and hurricane intensification in a barotropic model. *J. Atmos. Sci.,* **56,** 1674–1687.

——, and M. T. Montgomery, 2000: Tropical cyclone evolution via potential vorticity anomalies in a three-dimensional balance model. *J. Atmos. Sci.,* **57,** 3366–3387.

Montgomery, M. T., and R. J. Kallenbach, 1997: A theory for vortex Rossby waves and its application to spiral bands and intensity changes in hurricanes. *Quart. J. Roy. Meteor. Soc.,* **123,** 435–465.

——, and C. Lu, 1997: Free waves on barotropic vortices. Part I: Eigenmode structure. *J. Atmos. Sci.,* **54,** 1868–1885.

——, and J. Enagonio, 1998: Tropical cyclogenesis via convectively forced vortex Rossby waves in a three-dimensional quasigeostrophic model. *J. Atmos. Sci.,* **55,** 3176–3207.

——, J. D. Möller, and C. T. Nicklas, 1999: Linear and nonlinear vortex motion in an asymmetric balance shallow water model. *J. Atmos. Sci.,* **56,** 749–768.

Nolan, D. S., and B. F. Farrell, 1999: The intensification of two-dimensional swirling flows by stochastic asymmetric forcing. *J. Atmos. Sci.,* **56,** 3937–3962.

Obukhov, A. M., 1949: On the question of the geostrophic wind (in Russian). *Izv. Akad. Nauk SSSR Ser. Geogr. Geofiz.,* **13,** 281–306.

Reasor, P. D., and M. T. Montgomery, 2001: Three-dimensional alignment and co-rotation of weak, TC-like vortices via linear vortex Rossby waves. *J. Atmos. Sci.,* in press.

Reznik, G. M., and W. K. Dewar, 1994: An analytical theory of distributed axisymmetric barotropic vortices on the β-plane. *J. Fluid Mech.,* **269,** 301–321.

Ritchie, E. A., and G. J. Holland, 1993: On the interaction of tropical-cyclone-scale vortices. II: Discrete vortex patches. *Quart. J. Roy. Meteor. Soc.,* **119,** 1363–1379.

——, and ——, 1997: Scale interactions during the formation of Typhoon Irving. *Mon. Wea. Rev.,* **125,** 1377–1396.

Rossby, C. G., 1937: On the mutual adjustment of pressure and velocity distribution in simple current systems. *J. Mar. Res.,* **1,** 15–28.

Sadourny, R., 1975: The dynamics of finite-difference models of the shallow-water equations. *J. Atmos. Sci.,* **32,** 680–689.

Schecter, D. A., and D. H. E. Dubin, 1999: Vortex motion driven by a background vorticity gradient. *Phys. Rev. Lett.,* **83,** 2191–2194.

——, ——, A. C. Cass, C. F. Driscoll, I. M. Lansky, and T. M. O'Neil, 2000: Inviscid damping and growth of asymmetries on a 2D vortex. *Phys. Fluids,* **12,** 2397–2412.

Schubert, W. H., 1985: Wave, mean-flow interactions and hurricane development. Extended Abstracts, *16th Conf. on Hurricanes and Tropical Meteorology,* Houston, TX, Amer. Meteor. Soc., 140–141.

——, J. J. Hack, P. L. Silva Dias, and S. R. Fulton, 1980: Geostrophic adjustment in an axisymmetric vortex. *J. Atmos. Sci.,* **37,** 1464–1484.

Shapiro, L. J., and M. T. Montgomery, 1993: A three-dimensional balance theory for rapidly rotating vortices. *J. Atmos. Sci.,* **50,** 3322–3335.

Smith, G. B., and M. T. Montgomery, 1995: Vortex axisymmetrization: Dependence on azimuthal wave-number or asymmetric radial structure changes. *Quart. J. Roy. Meteor. Soc.,* **121,** 1615–1650.

Soules, S. D., and K. M. Nagler, 1969: Two tropical storms viewed by *Apollo 7. Bull. Amer. Meteor. Soc.,* **50,** 58–65.

Sutyrin, G. G., 1989: Azimuthal waves and symmetrization of an intense vortex. *Sov. Phys. Dokl.,* **34,** 104–106.

Trier, S. B., W. C. Skamarock, M. A. LeMone, and D. B. Parsons, 1996: Structure and evolution of the 22 February 1993 TOGA COARE squall line: Numerical simulations. *J. Atmos. Sci.,* **53,** 2861–2886.

Washington, W. M., and C. L. Parkinson, 1986: *An Introduction to Three-Dimensional Climate Modeling.* University Science Books, 422 pp.

Weisman, M. L., W. C. Skamarock, J. B. Klemp, and C. Davis, 1993: The generation of mesoscale convective vortices within long-lived convective systems. Preprints, *20th Conf. on Hurricanes and Tropical Meteorology,* San Antonio, TX, Amer. Meteor. Soc., 120–123.

Zehr, R., 1992: Tropical cyclogenesis in the western North Pacific. NOAA Tech. Rep. NESDIS 61, 181 pp. [Available from NOAA/NESDIS, The Regional and Mesoscale Team, gosden@cira.colostate.edu.]